

Dear Reviewer,

We would like to thank you for your constructive and helpful comments, which helped us to improve our manuscript. Significant changes have been made according to your comments and suggestions.

The following is our point-by-point response. The reviewer's comments are shown in *blue italics*. Our responses are provided in **black**. The revised text is in **red**.

Sincerely,

All of the authors

Reviewer #1

Intraseasonal variation of snow cover over Tibetan Plateau is very important for the prediction of surrounding and downstream regions. Recognizing the subseasonal prediction skill of TP snow cover in the current models are crucial for correcting and improving subseasonal prediction. Snow cover's S2S skill is scarcely studied, which is worthwhile to investigate. However, the current version has large space to improve. I suggest the resubmission after reframing the writing and clarifying the following points.

1. The writing frame should be modified. e.g., a. a method part should introduce the major method how to evaluate the S2S skill; b. the numerical experiment design and modeling introduction should be put earlier in this manuscript.

Response:

Good suggestions. Your suggested writing frame looks much more logic and clear. In the revised manuscript, Section 2 is now “2 Data and method”, which contains “2.1 S2S forecast models”, “2.2 Validation data and method”, “2.3 Numerical model and experimental design”.

2. The evaluation method of S2S skill is conventional and simple. To me, the major contribution of this study is intentionally S2S evaluation. therefore, please give some quantitative evaluation rather than only TCC.

Response:

Following your suggestions, three evaluation metrics, including the temporal correlation coefficient (TCC), the root-mean-square error (RMSE), and the mean bias are used to quantify the subseasonal forecast skill of TPSC in the state-of-the-art S2S models in the revised manuscript. In addition to these simple metric assessments, a composite analysis for increasing and decreasing TPSC cases is performed to further understand what leads to the forecast biases, which is crucial for model developers and users. Spatial pattern of systematic biases of TPSC for each grid points have also been provided in the revised manuscript.

3. What season of this study is focused on? I cannot find any information for this. Meanwhile, I guess the S2S prediction skill should have large seasonal dependence even monthly dependence. Please check.

Response:

Many thanks for your comments. This issue was also raised by Reviewer #2. We actually intended to focus on TPSC assessment in boreal winter, but our presentation in the original manuscript might not be clear and cause some confusion. Unlike the systematic biases of wintertime TPSC revealed by the S2S models, the forecast errors in summer are not consistent and show complex structures among different models. Thus, we focus on only the winter season in the current study and will leave the issues about summertime TPSC prediction for our future work.

4. Regional modeling portion, I cannot understand it very well. To me, one is the predicted lateral boundary layer, the other is observational boundary layer, of course the latter is better than the former. I don't know which point does this study want to present through the numerical modeling.

Response:

The relationship between snow cover and the atmosphere is a two-way coupling connection. Model sensitivity experiment is a good tool to clarify cause and effect. By designing and conducting the model experiments, we attempted to verify whether the cold SAT biases predicted by S2S models were caused by the overestimation of TPSC (instead of the opposite condition that the cold SAT leads to overestimated TPSC). Therefore, we used the predicted TPSC as boundary condition in CTL runs (with overestimated TPSC), while observational TPSC in

GDAS was used as boundary condition in EXP runs (without overestimated TPSC). We clarified the purpose why we carried out the numerical experiments in the revised manuscript.

“To reveal the causality of the systematic bias of the TPSC-induced regional SAT bias, numerical experiments are performed.” (in the revised Section 2)

“Through the results in Sections 4.1 and 4.2, we find that the local SAT over the Tibetan Plateau becomes colder with increasing forecast lead time. We assumed that the cold SAT biases are induced by the overestimation of TPSC. However, the relationship between snow cover and the atmosphere is a two-way coupling connection. The assumption should be tested by numerical experiments (see Section 2.2 for details about the numerical model and experimental design). Otherwise, one may suspect that the cold SAT induces an increasing TPSC other than the TPSC influence on SAT. Therefore, we used the predicted TPSC as boundary condition in CTL runs (with overestimated TPSC), while observational TPSC in GDAS was used as boundary condition in EXP runs (without overestimated TPSC). The difference between CTL and EXP is considered to represent the response or the sensitivity of the SAT to the overestimated TPSC.” (in the revised Section 4)

5. To fit “Cryosphere”, which is high-quality journal, at least, some physical analysis are needed. e.g., land-air budget analysis (surface fluxes) should be added to interpret the linkage between snow cover and surface temperature.

Response:

Excellent comments. We diagnosed the surface energy budget equation (Fig. 11c in the revised manuscript), the results of which indeed provides insightful explanations of TPSC-SAT relationship.

“By checking the land surface energy fluxes over the TP between CTL and EXP (Fig. 11c), we found that the overestimated TPSC strongly increases the upward-reflected shortwave radiation due to the snow-albedo affect. This difference in the solar surface energy leads to a decrease in the absorbed solar radiation. Thus, the net shortwave radiation is decreased (-10.2 W m^{-2}), while the response of the net longwave radiation is much smaller than that of the net shortwave radiation. The decreased absorbed solar radiation is mainly emitted by the land surface as sensible heat flux (-8.1 W m^{-2}). In contrast, the differences in the latent heat flux and ground heat flux are low. The overall responses of the surface energy to the overestimated TPSC lead to an incorrect cooling shift.” (in the revised Section 4)

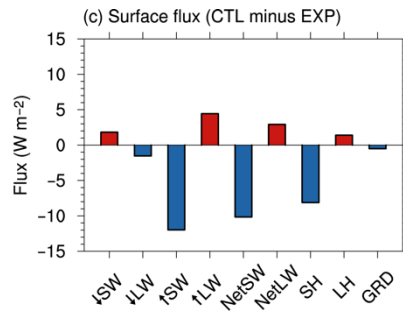


Figure 11c in the revised manuscript. Sensitivity of surface energy balance to TPSC biases in the numerical experiments. The difference in the surface energy balance between the CTL and EXP (CTL minus EXP) at 3 weeks in the numerical experiments. The terms from left to right are downward shortwave radiation (\downarrow SW), downward longwave radiation (\downarrow LW), upward shortwave radiation (\uparrow SW), upward longwave radiation (\uparrow LW), net shortwave radiation (NetSW), net longwave radiation (NetLW), sensible heat flux (SH), latent heat flux (LH) and ground heat flux (GRD) at the surface over the TP, respectively (unit: W m^{-2}).

Dear Reviewer,

We would like to thank you for your constructive and helpful comments, which helped us to improve our manuscript. Significant changes have been made according to your comments and suggestions.

The following is our point-by-point response. The reviewer's comments are shown in *blue italics*. Our responses are provided in **black**. The revised text is in **red**.

Sincerely,

All of the authors

Reviewer #2

This paper examines how a set of state-of-the-art subseasonal-to-seasonal (S2S) forecast systems predict the Tibetan Plateau-wide snow cover and surface temperature over the 1999-2010 period. The forecast systems from ECMWF, CMA and NCEP are used in the intercomparison. The evaluation of forecasted snow cover is made against the multi-instrument (IMS) snow cover data. A connection is drawn between the bias in snow cover, which increases systematically with lead time in all models, and a bias in surface temperature. Model experiments with the WRF model support the idea that the latter is induced by the snow excess through land-atmosphere coupling. Few papers have examined snow forecast on the S2S time scale on the Tibetan Plateau (TP), a region with well-known biases in snow and surface temperature. This is an innovative study that is well-worthy of publication in The Cryosphere. I however recommend a major revision of the paper, before it is in an acceptable form for publication.

MAJOR COMMENTS

1) Some brief description of how the three different models are initialised in terms of snow and land surface is needed, complementing the description of the land-surface models. What sort of snow analysis is used to initialise the different models? Isn't ERA-5, which has strong snow biases over the TP, used to initialise the ECMWF S2S reforecasts? Which observations are used in these snow analyses, both globally and over the TP more specifically? While IMS is not used to

initialise the ECMWF forecast model over the TP (see Orsolini Y. et al., 2019), is it used in the other systems? The quality of this initialisation would most certainly influence the snow forecasts at the S2S time scale. The initial snow values may be a key addition to bring in Fig 3.

Response:

Thank you for the useful comments. We completely agree with the reviewer that the information of snow initializations in S2S reforecasts has to be described clearly because they are the key factors influencing the TPSC prediction – the topic of our study. With a careful check, we confirmed that the northern hemisphere IMS snow cover data and ground observations of the snow depth available on the Global Telecommunications System (GTS) are used to initialize snow in the ECMWF S2S model. This is different from snow initialization in the ERA-5. Descriptions of snow initializations in the S2S forecasts were added in revised manuscript.

“For the ECMWF model, realistic snow is initialized in the forecasts. The snow mass is initialized by the ECMWF Land Data Assimilation System (LDAS). The snow initialization relies on a land surface synoptic report and national ground observations of the snow depth available on the Global Telecommunications System (GTS), as well as on the Interactive Multisensor Snow and Ice Mapping System (IMS) snow cover information. The NCEP model also initialize realistic snow in the forecasts. The snow initialization comes from the Climate Forecast System Reanalysis snow analysis using IMS and the Air Force Weather Agency snow depth analysis. Snow in the CMA model was not directly initialized in the forecasts. The initial conditions of the snow in the CMA model are from a balanced state produced by long-term air-sea initialization integration. See the details on snow initialization in the S2S models at <https://confluence.ecmwf.int/display/S2S/Models>.” (in the revised Section 2)

2) Some more details about how the snow cover fraction conversion is derived in each model is needed. For example, a 100% snow cover may mean very different snow depth or snow water equivalent (the actual prognostic variables) in the different prediction systems. Also, I believe that IMS provides a binary information snow cover being 0 or 1, with the former case meaning that the fractional snow cover is below 50%. When aggregated to a 1-degree grid (L88), isn't there a range or uncertainty in the IMS aggregated value (given that the observed fractional snow cover could actually be 0 or 50%)? Please clarify these points and the implications for forecast verification.

Response:

1. We added detailed descriptions about how the snow cover fraction conversion is derived in each model in the revised Section 2.1.

“According to the snow scheme in each land surface model, we obtain the snow cover fraction, which is a diagnostic variable in this study.

The snow cover fraction (f_{snow}) in the ECMWF model is parameterized as follows:

$$f_{\text{snow}} = \min[1, S/(0.1 \times \rho)] \quad (1)$$

where \min indicates the minimum function, S is the snow water equivalent (unit is kg m^{-2}), and ρ is the snow density (unit is kg m^{-3}) (Dutra et al., 2010).

The f_{snow} in the NCEP model is parameterized as follows:

$$f_{\text{snow}} = \min[1, 1 - (e^{-0.001 \times 2.6 \times S/SNUP} - 0.001 \times S/SNUP \times e^{-2.6})] \quad (2)$$

where e is the natural logarithm, and $SNUP$ is the vegetation parameter, which indicates the threshold snow depth (in water equivalent m) that implies 100% snow cover (Koren et al., 1999; Ek et al., 2003). The $SNUP$ ranges from 0.01 to 0.08 for different vegetation types. Details on the Noah code and vegetation parameters can be accessed in <https://ral.ucar.edu/solutions/products/unified-noah-lsm>.

The f_{snow} in the CMA model is parameterized as follows:

$$f_{\text{snow}} = \min[1, 1.77 \times d/(d + 10.6)] \quad (3)$$

where d is the snow depth (unit is cm), which is calculated from the snow water equivalent and snow density (Wu and Wu, 2004).”

2. We used a method similar to Orsolini (2019) to aggregate a 24-km resolution IMS analysis, which is interpolated into the $1^\circ \times 1^\circ$ grid of the S2S models. Details are provided in revised Section 2.2.

“The original 24-km resolution IMS analysis is interpolated into the $1^\circ \times 1^\circ$ grid of the S2S models. IMS provides binary snow cover information: it has the value of 1 if more than 50% of the 24-km pixel is covered by snow; otherwise, it is 0 (snow free). Orsolini et al. (2019) aggregated the original IMS product to a lower resolution rectilinear grid. They counted the number of pixels with a value of 1 in a grid box; assuming that they have 100% cover gave the high estimate, and assuming that they represent 50% cover gave the low estimate. These two estimates provide a range of values, which reflects the uncertainty inherent to aggregating the 24-km binary data, e.g., a value of 1 in a pixel means a 50% to 100% snow coverage. Here, we

used a method similar to Orsolini et al. (2019) to interpolate the original IMS product into the $1^{\circ}\times 1^{\circ}$ grid of S2S products, but we further averaged these two estimates.”

3) *The authors consider the snow cover averaged over the entire Tibetan-Plateau, but they do not show any snow cover maps although there is considerable heterogeneity, as shown by the authors in previous publications. I wonder if there could be compensation effects between different geographical sub-regions, that could result in an agreement of the TPSC index between forecasts and IMS. Different prediction systems may have different regional biases. Showing such maps would re-assure the reader that the prediction systems capture the main climatological features of the snow distribution over the TP and its S2S variability (e.g., in subregions as in Li W. et al., IJOC, 2019). Could spatial pattern correlation between IMS and snow forecasts be helpful in this case?*

Response:

Good suggestions. We plotted additional figures in the revised manuscript to show the spatial pattern of the systemic bias (Fig. 4 in the revised manuscript), as suggested by the reviewer.

“Taking the differences between the forecasts with a lead of 4 weeks and the forecasts with a lead of 1 week as an example, the spatial patterns of these increases in the biases in the three models show some similarities (Fig. 4). Although the spatial patterns of the differences in the three models show some small discrepancies, the differences are mainly positive in the three models, especially over parts of central and eastern Tibetan Plateau. These indicate that the increasing TPSC with the forecasting lead time are at a regional spatial scale.” (in the revised Section 3)

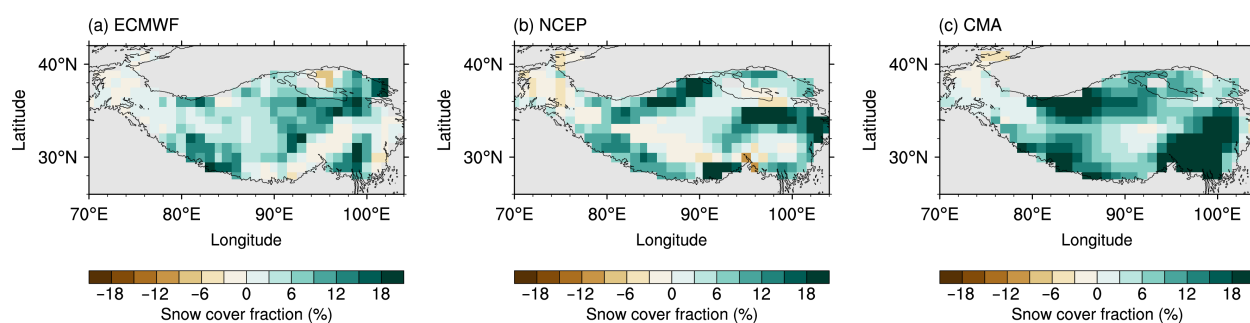


Figure 4 in the revised manuscript. Differences in the multiyear wintertime mean Tibetan Plateau snow cover fraction (unit: %) between forecasts with a lead of 4 weeks and forecasts with a lead of 1 week in (a) ECMWF, (b) NCEP and (c) CMA.

4) The authors could also try to examine the snow-temperature coupling strength (as an C2 indicator of land-atmosphere interaction) in the respective prediction systems by correlating the local forecasted temperature and forecasted snow, as a function of lead time. See Diro and Lin (2020) or Li et al. (2019).

Diro, G. T., and H. Lin, 2020: Subseasonal Forecast Skill of Snow Water Equivalent and Its Link with Temperature in Selected SubX Models. *Wea. Forecasting*, 35, 273–284.

Orsolini, Y., et al. G. (2019), Evaluation of snow depth and snow cover over the Tibetan Plateau in global reanalyses using in situ and satellite remote sensing observations. *The Cryosphere*, Vol. 13.(8) s.2221-2239

Li, F., et al. (2019). Impact of snow initialization in subseasonal to seasonal winter forecasts with the Norwegian Climate Prediction Model. *Journal of Geophysical Research: Atmospheres*, 124. <https://doi.org/10.1029/2019JD030903>

Response:

Many thanks for your good suggestion. The temporal correlations between snow cover fraction and SAT with forecast lead times of 1 week and 4 week for each grid point in three models were computed to identify the extent and nature of the snow-temperature relationship (Fig. 7 in the revised manuscript).

“The local SAT over the Tibetan Plateau is highly correlated with simultaneous TPSC at a subseasonal time scale (Li et al., 2020a). Local snow-temperature relationships in S2S models were examined. We took a similar approach as in F. Li et al. (2019) and Diro and Lin (2020). The temporal correlation between the snow cover fraction and SAT with a lead of 1 week and 4 weeks for each grid point in the three models was computed to identify the extent and nature of the relationship (Fig. 7). Almost all of the regions exhibit a significant negative correlation in all of these three models. Additionally, such a relationship in all three models did not weaken with the forecasting lead time (compare Fig. 7a–c and Fig. 7d–f), even if the forecasting skill on the TPSC declined over time. The reason is that the relationship between the snow cover fraction and the SAT is embedded in the land surface model.” (in the revised Section 4)

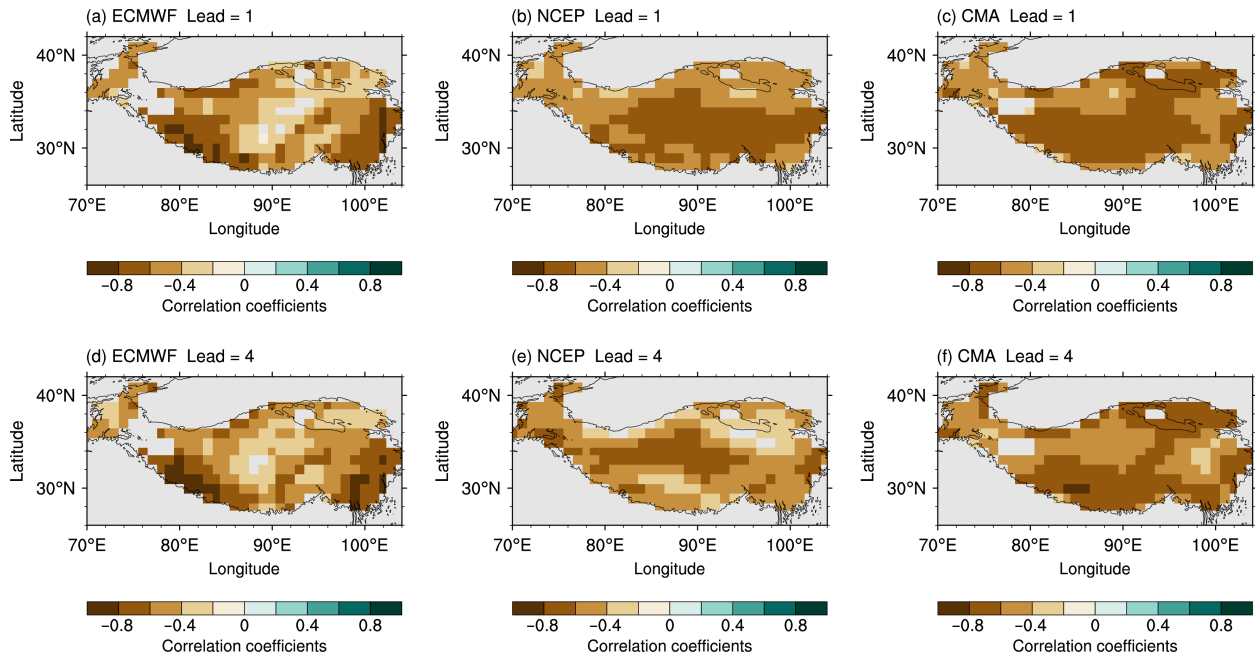


Figure 7 in the revised manuscript. Spatial pattern of correlations between the snow cover fraction and the surface air temperature with a lead of 1 week in (a) ECMWF, (b) NCEP and (c) CMA. Only significant correlations at the 0.01 level are displayed. (d)–(f) is similar to (a)–(c) but for forecasting with a lead of 4 weeks.

MINOR COMMENTS

L92-93: the description here focuses on winter. While winter is the main focus, many plots show year-long results. It would be better to emphasize the whole set used (nb of years, total nb of forecasts, . . .), not only the winters.

Response:

We are very sorry for the confusion. This issue is also raised by Reviewer #1. In fact, we attempted to focus on the TPSC study only for boreal winter considering that the TPSC biases during summer are not consistent among different models and there might have some complex processes involved. We have clarified the season that our present study focuses on and will leave the investigation of summertime TPSC prediction for our future work.

L252: the snow bias might not only arise from the land surface model (shared between WRF and the NCEP model) but also from the meteorological forcing (e.g., excess precipitation). Please clarify.

Response:

Motivated by this useful suggestion, we analyzed the precipitation in the forecast data and found that models tend to predict excess precipitation. The overestimated precipitation can explain why predicted snow cover increases with forecast lead times (Fig. 6 in the revised manuscript).

“Studies have shown that current state-of-the-art atmospheric general circulation models (GCMs) tend to strongly overestimate the precipitation over the Tibetan Plateau (e.g., Su et al., 2013; Chen and Frauenfeld, 2014; Zhang et al., 2016; Zhang et al., 2019). For example, Su et al. (2013) evaluated 24 GCMs that were available in the fifth phase of the Coupled Model Intercomparison Project (CMIP5) over the eastern Tibetan Plateau by comparing the model outputs with ground observations, and they found that all of the models consistently overestimated the observed precipitation for all seasons. Zhang et al., (2019) found similar results, in that all climate models they evaluated exaggerated the daily precipitation in the Tibetan Plateau during winter compared with the observed values. Here, we also found that the S2S models tended to overestimate the precipitation over the Tibetan Plateau. We compared the precipitation in the S2S models with both the gauges-based GPCP precipitation dataset and the satellite-based TRMM precipitation dataset (Fig. 6). The regional averaging wintertime mean precipitation over the Tibetan Plateau in the GPCP and TRMM models are 0.27 mm day^{-1} and 0.32 mm day^{-1} , respectively. Compared with the observed precipitation, all three S2S models exaggerate the regional precipitation obviously. Notably, such exaggerations always exist throughout the model integration. The ECMWF model reproduces the precipitation that is closest to the observations among the three models, but it still shows a large overestimation. The precipitation in the ECMWF model is 0.78 mm day^{-1} to 0.88 mm day^{-1} . The precipitation values in the NCEP model (1.07 mm day^{-1} to 1.37 mm day^{-1}) and in the CMA model (1.50 mm day^{-1} to 2.13 mm day^{-1}) have larger precipitation biases and even increase with the forecasting lead time. These overestimations of the precipitation induce underestimations of the TPSC dissipation, and they lead to positive biases in the TPSC from the models. Because the overestimation of the precipitation exists throughout the model integration, the positive biases of the TPSC accumulate and increase with the model integration.” (in the revised Section 3)

“All of the three S2S models consistently exaggerate the precipitation over the Tibetan Plateau compared to the observations. The exaggeration of the precipitation is prominent and always exists throughout the model integration. Systematic bias in the TPSC therefore occurs and accumulates with the model integration time due to exaggeration of the precipitation in the models.” (in the revised Section 5)

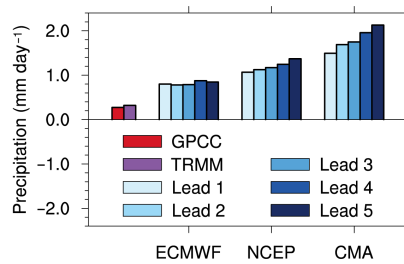


Figure 6 in the revised manuscript. The multiyear wintertime mean precipitation over the Tibetan Plateau (unit: mm day⁻¹) for the observations and forecasts in each model.

L244: how is the GDAS snow analysis used in Section 4.3 on numerical modelling compare with the IMS snow analysis, used in the first part of the paper. While it is mentioned that GDAS assimilates IMS, does it assimilate it over the TP? What does it assimilate specifically over the TP (in-situ data?)? Would the prediction skill be different if evaluated against GDAS (Fig 1) ?

Response:

The main conclusion in this study is that there is a systematic positive bias in the TPSC, and this bias increases with forecast lead times. To support this conclusion, the multiyear winter mean TPSC derived from the S2S models are compared to the observations.

Following your suggestion, we checked the multiyear winter mean TPSC in the GDAS (the FNL analyses). The multiyear winter mean TPSC index is 28.5% in the FNL analyses, and 31.9% in the IMS analyses. Compared to the systematic bias of TPSC in S2S models presented in this study, the difference of winter mean TPSC index between the FNL and the IMS are much smaller and do not change the main conclusion.

Conclusions: a brief mention of possible, relevant physical processes over the TP leading to snow ablation would be helpful. Could it be the strong surface winds or else the snow sublimation missing in the models? The short length of the period over which the forecasts are evaluated (around 10 years) is a bit of a concern. It appears that the biases are quite strong and systematic, but I wonder if some features in the forecasts would be robust over a longer period: for example, the slowdown in TPSC in early winter (December) seen in ECMWF and NCEP (Fig 3). I realise that if adding another 10 years may entail a lot of computational work, but it would add to the robustness of the conclusions. At least, a word of caution in the summary is warranted.

Response:

1. In the conclusion, we ascribed the sources of the systematic bias of TPSC prediction could come from the biased precipitation in the models. We agree with the reviewer that the

surface winds and snow sublimation could also play a role in causing the snow ablation. Identifying the relative contributions of these factors to the biased snow prediction needs more detailed and careful diagnoses. A discussion was added in Section 5. “Surface winds and snow sublimation could also play a role in causing the snow ablation. Identifying the relative contributions of these factors to the biased snow prediction needs more detailed and careful diagnoses. Future studies on this issue are potentially valuable.” We will address this issue in the near future. Thank you for your comments.

2. We conducted another 10 years of numerical experiments. The experiments in the revised manuscript ran for 20 winters (from 2000/2001 to 2019/2020).

Typos / English

L43: hydrologic cycle

L28: radiative rather than radiant

L108: the total variability

L113: and the three different

L143: the preceding week rather than the last week, seems more appropriate

L152: accumulation, leading to a systematic TPSC bias.

L168: growth is used for a declining variable. Either decrement, reduction or decline should be clearer.

L173: real rate should be observed rate or rate derived from IMS.

L173: indices or index

L202: growth of SAT, rather than TPSC (it says 1.2 degree).

L229: land-atmosphere interactions

L256: Hence,

Response:

All of these are corrected. We thank the reviewer for your careful reading of the manuscript.

Systematic bias of Tibetan Plateau snow cover in subseasonal-to-seasonal models

~~Shuzhen Hu⁺~~, Wenkai Li¹, [Shuzhen Hu¹](#), [Pang-chi Hsu¹](#), [Weidong Guo²](#), [Jiangfeng Wei¹](#)

¹Key Laboratory of Meteorological Disaster, Ministry of Education (KLME)/Joint International Research Laboratory of Climate and Environment Change (ILCEC)/Collaborative Innovation Center on Forecast and Evaluation of Meteorological Disasters (CIC-FEMD), Nanjing University of Information Science & Technology, Nanjing, 210044, China

²[Institute for Climate and Global Change Research, School of Atmospheric Sciences, Nanjing University, Nanjing, 210023, China](#)

10 *Correspondence to:* Wenkai Li (wenkai@nuist.edu.cn)

Abstract. Accurate subseasonal-to-seasonal (S2S) atmospheric forecasts and hydrological forecasts have considerable socioeconomic value. This study conducts a multimodel comparison of the Tibetan Plateau snow cover (TPSC) prediction skill using three models (ECMWF, NCEP and CMA) selected from the S2S project database to understand their performance in capturing TPSC variability [during wintertime](#). S2S models can skilfully forecast TPSC within a lead time of 2 weeks but show limited skill beyond 3 weeks. Compared with the observational snow cover analysis, all three models tend to overestimate the area of TPSC, ~~especially during winter~~. Another remarkable issue regarding the TPSC forecast is the increasing TPSC with forecast lead time, which further increases the systematic positive biases of TPSC in the S2S models at longer forecast lead times. ~~The underestimation of TPSC dissipation induces an increase in TPSC with forecast lead time in the models.~~ [All three S2S models consistently exaggerate the precipitation over the Tibetan Plateau. The exaggeration of precipitation is prominent and always exists throughout the model integration. Systematic bias of TPSC therefore occurs and accumulates with the model integration time.](#) Such systematic biases of TPSC influence the forecasted surface air temperature in the S2S models. The surface air temperature over the Tibetan Plateau becomes colder with increasing forecast lead time in the S2S models.

1 Introduction

Anomalous weather- and climate-related natural disasters are among the most common disasters and are associated with severe socioeconomic consequences. Reliable forecasts of such weather and climate anomalies with sufficient lead time have significant benefits for decision-makers (White et al., 2017). Traditionally, weather forecasts cover a time range of up to 2 weeks, while climate forecasts begin at the seasonal timescale and extend outward. Demands are growing rapidly in operational forecasts in the subseasonal-to-seasonal (S2S) range (from two weeks to a season). The primary basis for longer lead forecasts beyond 2 weeks is the interaction of the atmosphere with other, more slowly varying earth system components, such as the ocean or land, that evolve over timescales of weeks and months, rather than days as in the atmosphere (Mariotti et al., 2018).

Land–atmosphere coupling is one of the key physical processes for S2S prediction but is not well simulated and may reduce S2S prediction skill (Robertson et al., 2014; Dirmeyer et al., 2019).

Snow cover is a crucial component in both the climate system and the cryosphere. The [radiative](#) ~~radiant~~ and thermal properties of snow cover significantly influence the ground thermal regime (Zhang, 2005). As the lower boundary condition of the atmosphere, snow cover forces the regional and global atmosphere and can serve as an indicator of the atmosphere (Barnett et al., 1989; Bamzai and Shukla, 1999; Wu and Kirtman, 2007; Henderson et al., 2018). Snow cover can vary rapidly within a season over discontinuous or sporadic permafrost zones (Wang et al., 2015; Suriano and Leathers, 2018; Song et al., 2019; Li et al., 2020a) and rapidly influence the atmosphere (Clark and Serreze, 2000; Zhang et al., 2019). Snow cover may provide a potential source of S2S predictability via its variability and atmospheric effects at the subseasonal time scale ([F. Li et al., 2019](#); [Diro and Lin, 2020](#)).

The Tibetan Plateau is the highest plateau in the world and is known as the “third pole”. Due to its high elevation and cold climate, the Tibetan Plateau has much more snow cover than the other regions at the same latitude. Tibetan Plateau snow cover (TPSC) is a key component of the climate system. TPSC influences land surface thermal conditions (Chen et al., 2017; Li et al., 2018) and thus influences atmospheric circulations and monsoons over Asia and beyond (Wu and Qian, 2003; Lin and Wu, 2011; Xiao and Duan, 2016; Wang et al., 2017; You et al., 2020). TPSC shows variations at multiple time scales, including the subseasonal scale (Li et al. 2016; Song and Wu, 2019; Li et al., 2020a). The subseasonal variations in TPSC influence the atmosphere over East Asia (Li et al., 2018; Li et al., 2020b). A better [TPSC](#) simulation and ~~TPSC~~ forecast may favour a better forecast for weather and climate at the S2S time scale.

Snow cover also affects the [hydrologic](#) ~~hydrology~~ cycle. The accumulation of precipitation in the form of snow and its release through snowmelt runoff is an important component of the hydrologic cycle (Jeelani et al., 2012; Fayad et al., 2017). TPSC plays an important role in hydrological systems, providing a reservoir of water and acting as a buffer that controls river discharge. Rivers including the Yangtze River, Yellow River, Yarlung Zangbo River and Mekong River have headwaters over the Tibetan Plateau. Studies on the variability in TPSC are critical for water management in downstream regions (Immerzeel et al., 2009; Zhang et al., 2012; Zhang et al., 2013). Skilful predictions of TPSC with sufficient lead time are thus of great societal importance for hydrologic prediction.

Since the implementation of the S2S prediction project database (Vitart et al., 2016), many studies have evaluated the skill of S2S models for atmospheric elements and variables, such as the Madden–Julian Oscillation (Vitart, 2017), surface air temperature (Yang et al., 2018; Wulff and Domeisen, 2019), and precipitation (de Andrade et al., 2019). Some works also focus on the skill of S2S models for hydrological elements ([Wei Li et al., 2019](#); Schmitt Quedi and Mainardi Fan, 2020). However, we still know little about the skill of S2S models for TPSC. Understanding the forecasting skills of the S2S model on the TPSC is the first step to applying the S2S model to hydrological forecasts over the Tibetan Plateau. Moreover, considering the influence of TPSC on the atmosphere, clarifying the issue of the S2S model for TPSC helps improve the ability of the S2S model for atmospheric forecasting.

This study conducts a multimodel comparison of the TPSC prediction skill using selected models from the S2S project database to learn about their performance in capturing TPSC variability. Our main goal is to use the state-of-the-art S2S prediction systems of these operational centres to demonstrate why models exhibit systematic biases of TPSC and whether such systematic biases influence the regional air temperature forecasted in S2S models. The ~~remainder rest of the this~~ paper is organized as follows. Details on the data set [and method](#) used in this study are described in Section 2. The systematic bias of TPSC in S2S models and its effect on local temperature [during wintertime](#) are presented in Section 3 and Section 4, respectively. The conclusions and a discussion are presented in Section ~~65~~.

2 Data [and method](#)

[2.1 S2S forecast models](#)

The reforecasts considered for this study are taken from three operational forecast systems that are part of the S2S project database: the European Centre for Medium Range Weather Forecasts (ECMWF), the US National Centers for Environmental Prediction (NCEP), and the China Meteorological Administration (CMA). These models share a common reforecast period of 1999–2010 with a reforecast initialized frequency that is equal to or greater than once a week. This study only used reforecasts produced by the control forecast. Details of the S2S database can be found in Vitart et al. (2016). Daily reforecast data were averaged for each 7-day period starting every 1 January to create a total of 52 weeks per year (December 31 was excluded). The reforecasts that initialized on the first day of these weeks were selected. Forecast lead times were defined here as 1 week (1–7 days), 2 weeks (8–14 days), 3 weeks (15–21 days), 4 weeks (22–28 days), and 5 weeks (29–35 days).

[For the ECMWF model, realistic snow is initialized in the forecasts. The snow mass is initialized by the ECMWF Land Data Assimilation System \(LDAS\). The snow initialization relies on a land surface synoptic report and national ground observations of the snow depth available on the Global Telecommunications System \(GTS\), as well as on the Interactive Multisensor Snow and Ice Mapping System \(IMS\) snow cover information. The NCEP model also initialize realistic snow in the forecasts. The snow initialization comes from the Climate Forecast System Reanalysis snow analysis using IMS and the Air Force Weather Agency snow depth analysis. Snow in the CMA model was not directly initialized in the forecasts. The initial conditions of the snow in the CMA model are from a balanced state produced by long-term air-sea initialization integration. See the details on snow initialization in the S2S models at <https://confluence.ecmwf.int/display/S2S/Models>.](#)

The land surface models used for ECMWF, NCEP and CMA are the Hydrology Tiled ECMWF Scheme for Surface Exchanges over Land (HTESSEL; Balsamo et al., 2009), Noah (Ek et al., 2003) and BCC_AVIM2 (Wu et al., 2014), respectively. All these land surface models contain snow schemes. According to the snow scheme in each land surface model (~~Dutra et al., 2010; Koren et al., 1999; Wu and Wu, 2004~~), we obtain the snow cover fraction, which is a diagnostic variable in this study, ~~from the snow water equivalent and snow density~~.

~~The snow cover fraction (f_{snow}) in the ECMWF model is parameterized as follows:~~

$$f_{\text{snow}} = \min[1, S/(0.1 \times \rho)] \quad (1)$$

where min indicates the minimum function, S is the snow water equivalent (unit is $kg\ m^{-2}$), and ρ is the snow density (unit is $kg\ m^{-3}$) (Dutra et al., 2010).

The f_{snow} in the NCEP model is parameterized as follows:

$$f_{snow} = \min[1, 1 - (e^{-0.001 \times 2.6 \times S/SNUP} - 0.001 \times S/SNUP \times e^{-2.6})] \quad (2)$$

where e is the natural logarithm, and $SNUP$ is the vegetation parameter, which indicates the threshold snow depth (in water equivalent m) that implies 100% snow cover (Koren et al., 1999; Ek et al., 2003). The $SNUP$ ranges from 0.01 to 0.08 for different vegetation types. Details on the Noah code and vegetation parameters can be accessed in <https://ral.ucar.edu/solutions/products/unified-noah-lsm>.

The f_{snow} in the CMA model is parameterized as follows:

$$f_{snow} = \min[1, 1.77 \times d/(d + 10.6)] \quad (3)$$

where d is the snow depth (unit is cm), which is calculated from the snow water equivalent and snow density (Wu and Wu, 2004).

The surface air temperature (SAT) in these S2S models is also used. All variables are at a $1^\circ \times 1^\circ$ horizontal spatial resolution.

2.2 Validation data and method

The Tibetan Plateau area of focus in this study is the region within $26\text{--}41^\circ\text{N}$ and $70\text{--}105^\circ\text{E}$ at an altitude of greater than 3000 m (Fig. 1). Although the Tibetan Plateau is located over middle latitudes, the area is cold due to high altitude, especially in boreal winter. This study focuses on TPSC during wintertime. Here, each winter contains 17 weeks, covering from the 45th week (November 5–11) in one year to the 9th week (February 26–March 4) in the following year. This study spans 11 winters (from 1999/2000 to 2009/2010).

The reforecasts in the S2S models are verified against observational daily snow cover and SAT in the reanalysis. Observational daily snow cover data are obtained at a 24 km resolution from the Interactive Multisensor Snow and Ice Mapping System (IMS) snow cover analysis (Helfrich et al., 2007) provided by the National Oceanic and Atmospheric Administration. The IMS examines satellite images and other sources of data on snow cover and generates maps of snow cover distribution. The IMS analysis over the Tibetan Plateau corresponds well with ground-based measurements and can capture the general subseasonal variability in TPSC (Yang et al., 2015; Li et al., 2018). The original 24-km resolution IMS analysis is interpolated into the $1^\circ \times 1^\circ$ grid of the S2S models. IMS provides binary snow cover information: it has the value of 1 if more than 50% of the 24-km pixel is covered by snow; otherwise, it is 0 (snow free). Orsolini et al. (2019) aggregated the original IMS product to a lower resolution rectilinear grid. They counted the number of pixels with a value of 1 in a grid box; assuming that they have 100% cover gave the high estimate, and assuming that they represent 50% cover gave the low estimate. These two estimates provide a range of values, which reflects the uncertainty inherent to aggregating the 24-km binary data, e.g., a value of 1 in a pixel means a 50% to 100% snow coverage. Here, we used a method similar to Orsolini et al. (2019) to interpolate the original IMS product into the $1^\circ \times 1^\circ$ grid of S2S products, but we further averaged these two estimates. Daily SATs at a

1°×1° resolution are obtained from ERA-Interim reanalysis (Dee et al., 2011). These data range from 1 January 1999 to 30 December 2010. S2S reforecasts are compared with the observations and reanalysis for the same calendar date.

~~The Tibetan Plateau area of focus in this study is the region within 26–41°N and 70–105°E at an altitude of greater than 3000 m (Fig. 1). Although the Tibetan Plateau is located over middle latitudes, the area is cold due to high altitude, especially in boreal winter. This study mainly focuses on TPSC during wintertime. Here, each winter contains 17 weeks, covering from the 45th week (November 5–11) in one year to the 9th week (February 26–March 4) in the following year. This study spans 11 winters (from 1999/2000 to 2009/2010).~~

Two precipitation datasets, the Global Precipitation Analysis Products of the Global Precipitation Climatology Centre (GPCC; Schneider et al., 2011) and the Tropical Rainfall Measuring Mission (TRMM; Huffman et al., 2007), are used to evaluate the wintertime mean precipitation. The GPCC precipitation dataset is from rain-gauges built that were GTS-based. The TRMM precipitation dataset is based on satellite observations. The precipitation used in this study spans 11 winters (from 1999/2000 to 2009/2010).

To quantify the forecast ability of S2S models, three common statistical measures, i.e., the temporal correlation coefficient (TCC), the root-mean-square error (RMSE) and the mean bias, are calculated in this study. A composite analysis is performed to investigate the different performances on predicting the snow cover for increasing cases and decreasing cases (details are described in Section 3.2).

2.3 Numerical model and experimental design

To reveal the causality of the systematic bias of the TPSC-induced regional SAT bias, numerical experiments are performed. Numerical experiments are performed using the Advanced Weather Research and Forecasting Model (WRF-ARW, version 4.1.3), which was developed by the National Center for Atmospheric Research (NCAR). WRF-ARW has been applied to climate research, including studies of land-atmosphere interactions. The land surface parameterization scheme used in this study is the Noah land surface model (Ek et al., 2003). Important physics options include the WRF single-moment 6-class microphysics scheme (Hong and Lim, 2006), the NCAR Community Atmosphere Model (CAM 3.0) spectral-band shortwave and longwave radiation schemes (Collins et al., 2006), the Yonsei University planetary boundary layer scheme (Hong et al., 2006), and the Kain–Fritsch convective parameterization scheme (Kain, 2004). The WRF is driven by atmospheric and surface forcing data extracted from the National Centers for Environmental Prediction (NCEP) FNL Operational Model Global Tropospheric Analyses. The simulation domain is in a cylindrical Equidistant projection with a horizontal resolution of 1°×1° and located within 5–65°N and 40–170°E (as shown in Fig. 1).

Two ensemble experiments are performed: control (CTL) runs and sensitive experimental (EXP) runs. All these runs have the same initial times as the forecasts in the S2S models that we used in this study for each winter. But the experiments were run for 20 winters (from 2000/2001 to 2019/2020), and both runs contain 340 cases. Each member ran continuously for 22

165 days. The first day in each run is for spin-up, and the results are discarded. The CTL runs are integrated freely without any modification. Because both the NCEP S2S model and our numerical experiment use Noah as the land surface model, the TPSCs in CTL runs are expected to show unreal increases with integration time, which is similar to that in the NCEP S2S model (will be revealed in Section 3). The EXP run is designed to eliminate such bias in TPSC. The FNL analyses are from the Global Data Assimilation System (GDAS), which continuously collects observational data from the GTS and other sources for many analyses. GDAS incorporates daily snow data from IMS analyses and the Air Force Weather Agency Snow Depth Analysis Model. We replace the forecasted TPSC in the WRF model with TPSC in the FNL analyses every 6 hours. Because FNL analyses assimilate the observed TPSC, the TPSC in the EXP run is expected to show a small bias that increases with
170 integration time.

3 Tibetan Plateau snow cover in the S2S forecast models

3.1 Increasing Tibetan Plateau snow cover with forecast lead time

Before we present the systematic bias of TPSC in the S2S models, the overall forecast skills of TPSC is evaluated. Here, we focus on the variation in snow-covered area over the entire Tibetan Plateau, which can be measured by a TPSC index. The TPSC index represents the percentage of grid points covered by snow in the analysis or models over the entire Tibetan Plateau. The unit of the TPSC index is %. The prediction skill of the TPSC index has been investigated through the ~~temporal correlation coefficient~~ (TCC and RMSE) between the TPSC index in the predictions and that in the observations during wintertime (Fig. 2). A skilful prediction is generally defined as a TCC greater than 0.5. All three models show good prediction skills at lead times of 1–2 weeks with a TCC greater than 0.5 (Fig. 2a). At lead times of 1–2 weeks, the TCC for the ECMWF model is largest among the three models. The NCEP model has the lowest TCC among the three models at a lead time of 1 week. However, the TCC for NCEP falls the most slowly at lead times of 2 weeks or more. The NCEP model has a larger TCC than the CMA model at lead times of 2 weeks or more. The TCC values decrease with the increase in the forecast lead time and decline below 0.5 at and after lead times of 3 weeks for all three models. RMSEs increase with the forecast lead time (Fig. 2b). The RMSE for ECMWF is the smallest among the three models. Additionally, CMA has the largest RMSEs. These results
185 indicate that the S2S models can skilfully forecast TPSC variations within a lead time of 2 weeks during wintertime but show limited skill at a lead time of 3 weeks or more.

The above results also indicate that the ECMWF model is shown to have a better TPSC forecasting skill than the other two models. Even so, the ECMWF model shows nonnegligible RMSEs with a TPSC index of more than 15% (Fig. 2b). The other two models, especially the CMA model, show even more significant RMSEs up to more than 25%. These large errors in the forecasting of the TPSC are induced by systematic bias of the TPSC, as shown by the following. The multiyear wintertime mean biases of the TPSC index in forecasts against that in the IMS snow cover analysis for all three models show positive values, which indicates that all of the models tend to overestimate the TPSC during winter (Fig. 3a). The TPSC index in the
190

ECMWF is higher than the observed TPSC index by approximately 20–30%. NCEP has a larger TPSC index than that in the observation by approximately 5–20%. The CMA shows largest biases of approximately 25–40%.

~~The seasonal cycle of TPSC is generally the most dominant component that contributes to the total variabilities in TPSC (Li et al., 2020a). The prediction ability of models for the seasonal cycle of TPSC directly affects the prediction ability for the total variability in TPSC. Systematic bias of TPSC in models will also be exposed in their multi-year mean seasonal cycle. Because multi-year mean seasonal cycles of TPSC in the S2S models are based on only twelve years of available reforecasts in this study, a 90-day low-pass filter is performed on the raw multi-year mean seasonal cycle to eliminate the unnecessary high-frequency signal. The seasonal cycle of TPSC indexes in IMS and three different models show some obvious differences (Fig. 3). Models can generally reproduce the seasonal cycle of the TPSC index but with some non-negligible biases. Compared with the IMS analysis, all models tend to overestimate the TPSC index during winter. The TPSC index in the ECMWF is higher than the observed TPSC index by approximately 10–30% all-year round (Fig. 3a). NCEP has a larger TPSC index than that in the observation by approximately 10–30% during wintertime but tends to underestimate the TPSC index by approximately 10% during summertime (Fig. 3b). CMA overestimates the TPSC index all-year round (Fig. 3c), especially during winter and spring (up to 30%). Overall, overestimation of the TPSC area is common in models compared with observations, especially during winter.~~

Another remarkable issue regarding the forecast of TPSC is the increasing TPSC with forecast lead time, which further increases the overestimation of TPSC in models at longer forecast lead times. These increasing biases can be detected from the multiyear winter mean seasonal cycle biases (Fig. 3a). To highlight such increasing biases, we further present differences in the multiyear winter biases ~~mean seasonal cycle~~ for the TPSC index between forecasts for leads of 2–5 weeks and forecasts for leads of 1 week in three modes (Fig. 4b). Such differences are obtained by subtracting the multiyear winter mean of TPSC index ~~the seasonal cycle~~ at a lead time of 1 week from that at forecast lead times of 2–5 weeks. The differences in the three models show ~~some common features:~~ the differences in all three models are mainly all positive and increase with increasing forecast lead time except for some short periods during summertime. ~~By comparing values at different lead times, we found that such positive differences increase with increasing lead time. In general,~~ The positive biases of TPSC with the longest forecast lead time (5 weeks; red lines in Fig. 4) are largest among all forecasts in autumn, winter and spring. The increases in the differences in the ECMWF model are the smallest, while the CMA model has the largest increases in the differences. Taking the differences between the forecasts with a lead of 4 weeks and the forecasts with a lead of 1 week as an example, the spatial patterns of these increases in the biases in the three models show some similarities (Fig. 4). Although the spatial patterns of the differences in the three models show some small discrepancies, the differences are mainly positive in the three models, especially over parts of central and eastern Tibetan Plateau. These indicate that the increasing TPSC with the forecasting lead time are at a regional spatial scale.

The forecast results of each model also show some unique characteristics. The increase in the ECMWF bias peaks in autumn and is maintained through winter and spring, especially for that at a forecast lead time of 3–5 weeks (Fig. 4a). The increase in the NCEP bias shows large values during autumn and spring, but considerable values are still observed during winter (Fig. 4b). The increase in the CMA bias is similar to that in ECMWF but shows larger values than that in ECMWF (Fig. 4c). Overall, the systematic positive biases of TPSC in the S2S models increase with increasing forecast lead time during the cold season.

3.2 Snow cover accumulation versus dissipation

The intraseasonal variability in TPSC leads to obvious rapid variations in TPSC with a period shorter than a season, making TPSC exhibit a distinct lack of persistence within one season (Li et al., 2020a). Both accumulation and dissipation of snow cover occur within a season over the Tibetan Plateau. The increase in TPSC with forecast lead time in the models may be induced by overestimation of snow cover accumulation or underestimation of snow cover dissipation. To support this hypothesis, we analysed the frequency of weekly TPSC accumulation and dissipation in the observation and forecast models in winter (Table 1). Here, the increasing (decreasing) weeks means that the TPSC index is greater (less) than that in the preceding ~~last~~ week. The TPSC indexes in the S2S models are compared with the TPSC index in the preceding ~~last~~ week, which are initialized at the same time, but with different forecast lead times.

The proportions of increasing and decreasing weeks in the observations are 50.3% and 49.7%, respectively, which is fairly even (Table 1). However, this kind of balance does not exist in the models. In the models, the proportion of increasing weeks is mostly more than 2 times as large as the proportion of decreasing weeks. The proportion of decreasing weeks is low compared with that in the observations. Specifically, decreasing weeks occupy only 23.0–31.0% of the total forecasts by ECMWF. NCEP shows similar results, except for forecasting at a lead time of 5 weeks. This underestimation of the proportion of decreasing weeks is more severe in CMA. Moreover, the most severe underestimations of the proportion of decreasing weeks are the forecasts with a lead time of 2 or 3 weeks for all models.

The above results indicate that the models underestimate the frequency of TPSC dissipation, whereas they overestimate the frequency of TPSC accumulation, which leads to a systematic TPSC bias. ~~Then, systematic TPSC bias may occur and increase.~~ To highlight increases in the overall TPSC biases, as well as changes in biases in successive weeks, a composite analysis is performed for all TPSC reforecasts during winter (Fig. 5a), increasing TPSC cases (Fig. 5b) and decreasing TPSC cases (Fig. 5c). All reforecasts initialized in winter are taken into account for the composite of all cases shown in Fig. 5a. The sample numbers of all cases are 187. Among all cases, we further select the increasing TPSC cases and decreasing TPSC cases. If the TPSC index continues to increase (decrease) for three weeks, this case is regarded as an increasing (decreasing) TPSC case. There are 46 increasing TPSC cases and 53 decreasing TPSC cases. We average the 46 (53) cases for different lead times. To focus on the increase in biases, values with a lead time of 1 week are removed for forecasting at all lead times.

On a seasonal average, the growth of the TPSC index in winter is only 1.3% over two weeks in the observation (black line in Fig. 5a). However, the models tend to exaggerate the growth of the TPSC index (colour lines in Fig. 5a). The growth

of the TPSC index over the two weeks in the models ranged from 4.9% (ECMWF) to 9.8% (CMA). The TPSC index in the
260 forecast shows distinct differences between the increasing TPSC cases and decreasing TPSC cases (Fig. 5b and 5c). The growth
of the TPSC index in the increasing TPSC cases is 14.1% over two weeks in the observation (black line in Fig. 5b). The growth
of the TPSC index over two weeks in NCEP and CMA is close to that in the observation, while there is some underestimation
of such growth in the ECMWF (colour lines in Fig. 5b). Although there are some differences between the TPSC index in the
models and that in the observation, all models can forecast the increasing trend in the TPSC index. However, the situation for
265 the decreasing TPSC cases is quite different. The ~~reduction growth~~ of the TPSC index in the decreasing TPSC cases is -10.0%
over two weeks in the observation (black line in Fig. 5c). However, all the changes in the TPSC index in the models are positive
values (colour lines in Fig. 5c), indicating that there are some difficulties for the models in forecasting the dissipation of TPSC.

Studies have shown that current state-of-the-art atmospheric general circulation models (GCMs) tend to strongly
overestimate the precipitation over the Tibetan Plateau (e.g., Su et al., 2013; Chen and Frauenfeld, 2014; Zhang et al., 2016;
270 Zhang et al., 2019). For example, Su et al. (2013) evaluated 24 GCMs that were available in the fifth phase of the Coupled
Model Intercomparison Project (CMIP5) over the eastern Tibetan Plateau by comparing the model outputs with ground
observations, and they found that all of the models consistently overestimated the observed precipitation for all seasons. Zhang
et al., (2019) found similar results, in that all climate models they evaluated exaggerated the daily precipitation in the Tibetan
Plateau during winter compared with the observed values. Here, we also found that the S2S models tended to overestimate the
275 precipitation over the Tibetan Plateau. We compared the precipitation in the S2S models with both the gauges-based GPCC
precipitation dataset and the satellite-based TRMM precipitation dataset (Fig. 6). The regional averaging wintertime mean
precipitation over the Tibetan Plateau in the GPCC and TRMM models are 0.27 mm day^{-1} and 0.32 mm day^{-1} , respectively.
Compared with the overserved precipitation, all three S2S models exaggerate the regional precipitation obviously. Notably,
such exaggerations always exist throughout the model integration. The ECMWF model reproduces the precipitation that is
280 closest to the observations among the three models, but it still shows a large overestimation. The precipitation in the ECMWF
model is 0.78 mm day^{-1} to 0.88 mm day^{-1} . The precipitation values in the NCEP model (1.07 mm day^{-1} to 1.37 mm day^{-1})
and in the CMA model (1.50 mm day^{-1} to 2.13 mm day^{-1}) have larger precipitation biases and even increase with the
forecasting lead time. These overestimations of the precipitation induce underestimations of the TPSC dissipation, and they
lead to positive biases in the TPSC from the models. Because the overestimation of the precipitation exists throughout the
285 model integration, the positive biases of the TPSC accumulate and increase with the model integration.

In this section, it was found that S2S models underestimate the frequency of TPSC dissipation and have some difficulties
forecasting TPSC dissipation with an observed ~~real~~ rate. Exaggerations of the precipitation were found in all three models,
which directly lead to accumulated overestimation of TPSC. As a result, systematic bias of TPSC occurs and increases with
290 the model integration time. ~~the underestimations of TPSC dissipation induce an increase in TPSC with forecast lead time in
the models.~~

4 Sensitivity of local surface air temperature to snow cover biases

4.1 Colder temperature with increasing forecast lead time

295 The local SAT over the Tibetan Plateau is highly correlated with simultaneous TPSC at a subseasonal time scale (Li et al., 2020a). Local snow-temperature relationships in S2S models were examined. We took a similar approach as in F. Li et al. (2019) and Diro and Lin (2020). The temporal correlation between the snow cover fraction and SAT with a lead of 1 week and 4 weeks for each grid point in the three models was computed to identify the extent and nature of the relationship (Fig. 7). Almost all of the regions exhibit a significant negative correlation in all of these three models. Additionally, such a relationship
300 in all three models did not weaken with the forecasting lead time (compare Fig. 7a–c and Fig. 7d–f), even if the forecasting skill on the TPSC declined over time. The reason is that the relationship between the snow cover fraction and the SAT is embedded in the land surface model.

~~The skill of predicting the TPSC will further influence the skill of predicting the SAT. The variation in snow-covered area over the entire Tibetan Plateau immediately changes the local land surface albedo. The surface air temperature (SAT) is further influenced.~~
305 ~~As shown in Section 3, the TPSC in the S2S models during the cold season increases with increasing forecast lead time. Such systematic biases of TPSC may influence the forecasted SAT in the S2S models. To test this hypothesis, we performed an analysis on SAT over the Tibetan Plateau similar to our analysis on TPSC. The SAT over the Tibetan Plateau is derived by averaging the SAT over the Tibetan Plateau region as defined in Section 2.2. Differences in the multiyear winter mean seasonal cycles for SAT over the Tibetan Plateau between forecasts with leads of 2–5 weeks and forecasts with leads of~~
310 ~~1 week in the three models, which were obtained by subtracting the multiyear winter mean seasonal cycle with a lead time of 1 week from that for forecast lead times of 2–5 weeks, are examined (Fig. 8).~~

The differences in the three models show some common features. The differences in all three models are ~~mainly all~~
negative ~~except for some short periods during summertime~~. By comparing values at different lead times, we also find that such negative differences increase with increasing lead time, except for value at lead of 3 week in CMA model. The negative
315 differences of SAT with the longest forecast lead time (5 weeks, ~~red lines in Fig. 6~~) are largest among all forecasts ~~in autumn, winter and spring~~. The differences in SAT between the forecast for lead 5 weeks and the forecast for lead 1 week can be up to ~~1.8–9~~ °C. The increases in the SAT with the forecasting lead time are on a regional spatial scale (Fig. 9). Almost all of the grid points show negative values. Such increases in the CMA are less than those in ECMWF and NCEP.

~~Such differences in ECMWF are more obvious than those in NCEP and CMA.~~
320 ~~The above results indicate that the SAT over the Tibetan Plateau becomes colder with increasing forecast lead time in the S2S models. Considering the results we obtained in Section 3, it can be concluded that the increasing TPSC is accompanied by decreasing SAT with forecast lead time.~~

4.2 Sensitivity of SAT to snow cover accumulation and dissipation

Section 3.2 reveals that models show different performances on snow cover accumulation and dissipation. We also found that there are some difficulties for the models in forecasting the dissipation of TPSC. To learn whether such different performances

325 influence the SAT forecast and to examine the sensitivity of SAT to TPSC in the S2S models, we investigated the changes in SAT in the S2S models over the Tibetan Plateau during winter (Fig. [7a10a](#)), as well as the increasing TPSC cases (Fig. [107b](#)) and decreasing TPSC cases (Fig. [107c](#)). To provide a SAT reference in the models, a composite was performed on SAT in the ERA-interim reanalysis. We performed the same composite method as that is used in Section 3.2 on TPSC but for SAT over the Tibetan Plateau.

330 On a seasonal average, the change in SAT over the Tibetan Plateau in the reanalysis during winter is less than 0.1 °C (black line in Fig. [107a](#)). However, the SAT in the models tends to decrease as the forecast lead time increases, especially in the ECMWF and NCEP models (colour lines Fig. [107a](#)). The growth of the ~~SAT-TPSC index~~ over two weeks is 1.2 °C for the ECMWF and NCEP models. Considering the exaggerated growth of TPSC shown in Fig. 5a, a decrease in SAT is expected. In the ECMWF and NCEP models, more TPSC leads to lower SAT. SAT tends to be sensitive to TPSC in the ECMWF and
335 NCEP models. However, SAT in the CMA model lacks sensitivity to TPSC. Although the exaggerated growth of the TPSC index in the CMA model is the most intense in these three models, the decrease in SAT in the CMA model is the least obvious.

The change in SAT should be closely connected to the variations in TPSC. The change in SAT in the increasing TPSC cases is -1.9 °C in two weeks in the ERA-interim reanalysis (black line in Fig. [107b](#)), which is associated with the accumulation of TPSC (black line in Fig. 5b). SAT shows considerable decreases during the increasing TPSC cases (Fig. [107b](#)). Cold biases
340 of SAT between the forecasted SAT with lead time and that at the initial week tend to appear in all models (Fig. [107b](#)), which is associated with accumulation of TPSC (in Fig. 5b). Here, the change in SAT in CMA over two weeks is smaller than that in the ECMWF and NCEP models. SATs in the ECMWF and NCEP models are more sensitive to TPSC than that in the CMA model.

In Section 3.2, we found that there are some difficulties for the models in terms of forecasting the TPSC dissipation. Here,
345 we further find that such biases lead to biases in SAT. SAT increases by 1.4 °C over two weeks in the reanalysis (black line in Fig. [107c](#)), which is associated with the dissipation of TPSC (black line in Fig. 5c). However, the SATs in all these models shows small changes (colour lines in Fig. [107c](#)) compared with that in the reanalysis. Such small changes in the SATs in the ECMWF and NCEP models are consistent with the changes in the TPSC indexes in these models, which show little changes (Fig. 5c). However, the large change in TPSC in the CMA model (Fig. 5c) does not induce large biases in SAT, indicating that
350 the SAT in CMA lacks sensitivity to TPSC.

4.3 Numerical experiment

Through the results in Sections 4.1 and 4.2, we find that the local SAT over the Tibetan Plateau becomes colder with increasing forecast lead time. We assumed that the cold SAT biases are induced by the overestimation of TPSC. However, the relationship between snow cover and the atmosphere is a two-way coupling connection (Henderson et al., 2018). The assumption should
355 be tested by numerical experiments ([see Section 2.2 for details about the numerical model and experimental design](#)). Otherwise, one may suspect that the cold SAT induces an increasing TPSC other than the TPSC influence on SAT. [Therefore, we used the predicted TPSC as boundary condition in CTL runs \(with overestimated TPSC\), while observational TPSC in GDAS was](#)

used as boundary condition in EXP runs (without overestimated TPSC). The difference between CTL and EXP is considered to represent the response or the sensitivity of the SAT to the overestimated TPSC.

~~Numerical experiments are performed using the Advanced Weather Research and Forecasting Model (WRF-ARW, version 4.1.3), which was developed by the National Center for Atmospheric Research (NCAR). WRF-ARW has been applied to climate research, including studies of land-air interactions. The land surface parameterization scheme used in this study is the Noah land surface model (Ek et al., 2003). Important physics options include the WRF single-moment 6-class microphysics scheme (Hong and Lim, 2006), the NCAR-Community Atmosphere Model (CAM 3.0) spectral band shortwave and longwave radiation schemes (Collins et al., 2006), the Yonsei University planetary boundary layer scheme (Hong et al., 2006), and the Kain-Fritsch convective parameterization scheme (Kain, 2004). The WRF is driven by atmospheric and surface forcing data extracted from the National Centers for Environmental Prediction (NCEP) FNL-Operational Model-Global Tropospheric Analyses. The simulation domain is in a cylindrical Equidistant projection with a horizontal resolution of $1^\circ \times 1^\circ$ and located within $5^\circ\text{--}65^\circ\text{N}$ and $40^\circ\text{--}170^\circ\text{E}$ (as shown in Fig. 1).~~

~~Two ensemble experiments are performed: control (CTL) runs and sensitive experimental EXP runs. Both runs contain 187 forecasts. All these runs have the same initial times as the forecasts in the S2S models that we used in this study. Each member ran continuously for 22 days. The first day in each run is for spin-up, and the results are discarded. The CTL runs are integrated freely without any modification. Because both the NCEP S2S model and our numerical experiment use Noah as the land surface model, the TPSCs in CTL runs are expected to show unreal increases with integration time, which is similar to that in the NCEP S2S model. The EXP run is designed to eliminate such bias in TPSC. The FNL analyses are from the Global Data Assimilation System (GDAS), which continuously collects observational data from the Global Telecommunications System and other sources for many analyses. GDAS incorporates daily snow data from IMS analyses and the Air Force Weather Agency Snow Depth Analysis Model. We replace the forecasted TPSC in the WRF model with TPSC in the FNL analyses every 6 hours. Because FNL analyses assimilate the observed TPSC, the TPSC in the EXP run is expected to show a small bias that increases with integration time.~~

We averaged snow cover and SAT over the Tibetan Plateau in all simulations for CTL and EXP to obtain a composite for all reforecasts of TPSC during winter in the numerical experiment (Fig. [§11a–b](#)). As we discussed in Section 3.2, the growth of the TPSC index in winter is only 1.3% for two weeks in the observations, while the S2S models tend to exaggerate the growth of the TPSC index (Fig. 5a). In the numerical experiment, CTL also exaggerates the growth of the TPSC index (blue line in Fig. [§11a](#)). Because both the NCEP S2S model and our numerical experiment use Noah as the land surface model, such biases may be attributed to the land surface model. Compared with CTL, EXP shows smaller cumulative biases (red line in Fig. [§11a](#)), which is because TPSC in EXP is replaced by TPSC in the FNL analyses every 6 hours. The SAT becomes colder with increasing forecast lead time in CTL (blue line in Fig. [§11b](#)). However, such a decrease in SAT is much smaller in EXP (red line in Fig. [§11b](#)). By checking the land surface energy fluxes over the TP between CTL and EXP (Fig. 11c), we found that the overestimated TPSC strongly increases the upward-reflected shortwave radiation due to the snow-albedo affect. This difference in the solar surface energy leads to a decrease in the absorbed solar radiation. Thus, the net shortwave

radiation is decreased (-10.2 W m^{-2}), while the response of the net longwave radiation is much smaller than that of the net shortwave radiation. The decreased absorbed solar radiation is mainly emitted by the land surface as sensible heat flux (-8.1 W m^{-2}). In contrast, the differences in the latent heat flux and ground heat flux are low. The overall responses of the surface energy to the overestimated TPSC lead to an incorrect cooling shift. Hence ~~Here,~~ the numerical experiment indicates that the cold SAT biases are induced by the overestimation of TPSC.

5 Conclusions and discussion

Accurate subseasonal-to-seasonal (S2S) atmospheric forecasts and hydrological forecasts have considerable socioeconomic value. This study evaluates the Tibetan Plateau snow cover (TPSC) prediction capabilities of three S2S forecast models (ECMWF, NCEP and CMA) during wintertime. These three S2S models can skilfully forecast TPSC variations within a lead time of 2 weeks during wintertime with temporal correlation coefficients greater than 0.5. ECMWF better captures TPSC variations compared with NCEP and CMA at a lead time of 1–2 weeks. All models show limited skill in forecasting TPSC at a lead time of 3 weeks or more. Compared with the IMS snow cover analysis, all three models tend to overestimate the area of TPSC, ~~especially during winter~~. Another remarkable issue regarding the TPSC forecast is the increasing TPSC with forecast lead time, which makes the systematic positive biases of TPSC in models further increase at longer forecast lead times. ~~Generally, the positive biases of TPSC with the longest forecast lead time are largest among all forecasts with different lead times for most of the year.~~

S2S models underestimate the frequency of TPSC dissipation, whereas they overestimate the frequency of TPSC accumulation. The accumulation and dissipation of wintertime TPSC occurs evenly in the observations. However, this kind of balance does not exist in the S2S models. In the models, the proportion of TPSC accumulation is mostly more than 2 times as large as the dissipation proportion. The most severe underestimations of the dissipation proportions are the forecasts at a lead time of 2 or 3 weeks for all models. The models also have some difficulties forecasting the TPSC dissipation at a real rate. The growth of TPSC in the decreasing TPSC cases is -10.0% over two weeks in the observations, but all the changes in TPSC in the models are increasing. ~~As a result, the underestimation of TPSC dissipation induces an increase in TPSC with forecast lead time in the models.~~

All of the three S2S models consistently exaggerate the precipitation over the Tibetan Plateau compared to the observations. The exaggeration of the precipitation is prominent and always exists throughout the model integration. Systematic bias in the TPSC therefore occurs and accumulates with the model integration time due to exaggeration of the precipitation in the models.

The increasing TPSC is accompanied by decreasing surface air temperature (SAT) with forecast lead time. The SAT over the Tibetan Plateau becomes colder with increasing forecast lead time in the S2S models. ~~The negative differences in SATs with the longest forecast lead times are largest among all forecasts in autumn, winter and spring.~~ The differences in SATs between the forecast for a lead of 5 weeks and the forecast for a lead of 1 week can be up to $1.8\text{--}9^\circ\text{C}$. SATs tends to be sensitive

to the TPSCs in both ECMWF and NCEP. However, SAT in CMA lacks sensitivity to TPSC. Numerical experiments were performed to test whether the cold SAT biases are induced by the TPSC overestimation. The control run exaggerates the growth of TPSC, which is similar to that in S2S models. The SAT in the control run becomes colder with integration time. When the increasing TPSC with forecast lead time in the models along with the integration of the model is removed in the sensitivity run, ~~the overestimated snow cover in the numerical model is flattened. Meanwhile,~~ the decreasing SAT with integration time also disappears. [The overall responses of the surface energy to the overestimated TPSC lead to incorrect cooling shifts.](#) This finding indicates that cold SAT biases are induced by the TPSC overestimation.

Land-atmosphere coupling is one of the key physical processes for S2S prediction but is not well simulated and may reduce S2S prediction skill (Robertson et al., 2014; Dirmeyer et al., 2019). Studies have shown that better snow cover initialization improves subseasonal and seasonal forecasts/simulations (Jeong et al., 2013; Orsolini et al., 2013; Senan et al., 2016; Lin et al., 2016; Kolstad, 2017; [F. Li et al., 2019](#)). This study indicates that in addition to snow cover initialization, a better model skill for snow cover prediction may also improves S2S prediction skill. More work is necessary and valuable to improve the prediction ability of models for snow cover.

[Previous studies have shown that current state-of-the-art GCMs tend to strongly overestimate the precipitation over the Tibetan Plateau \(e.g., Su et al., 2013; Chen and Frauenfeld, 2014; Zhang et al., 2016; Zhang et al., 2019\). It is worthwhile to note that the S2S models also significantly overestimate the precipitation over the Tibetan Plateau and further cause other biases \(e.g., TPSC biases and SAT biases\). It is of great significance to reduce the biases of the precipitation over the Tibetan Plateau in the GCMs. Surface winds and snow sublimation could also play a role in causing the snow ablation. Identifying the relative contributions of these factors to the biased snow prediction needs more detailed and careful diagnoses. Future studies on this issue are potentially valuable.](#)

Data and code availability

The data and model used in this study are free to the public. The S2S datasets and ERA-interim data are available at <https://apps.ecmwf.int/datasets/>. The IMS snow cover data are available at <https://nsidc.org/data/G02156>. [The GPCC data are available at https://www.dwd.de/EN/ourservices/gpcc/gpcc.html. The TRMM data are available at https://disc.gsfc.nasa.gov.](#) The NCEP FNL data are available at <https://rda.ucar.edu/datasets/ds083.2/>. The WRF source codes can be obtained at https://www2.mmm.ucar.edu/wrf/users/download/get_source.html. All figures were produced using NCAR Command Language (NCL) version 6.6.2, an open source software free to the public, by UCAR/NCAR/CISL/TDD, <https://doi.org/10.5065/d6wd3xh5>. The NCL scripts used in this study are available from the corresponding author upon reasonable request.

Author contribution

455 W.L. led the overall scientific questions and designed the research. S.H. and W.L. analyzed the data and drafted the manuscript
[for initial submission. W.L. analyzed the data for the revised manuscript. W.L., P.H., W.G. and J.W. made substantial
contributions to revise the manuscript and prepare the responses to the referees.](#)

Competing interests

The authors declare no competing interests.

460 Acknowledgements

This research is supported by the National Key Research and Development Program of China (2018YFC1505804), Natural Science Foundation of China (41905074), the Natural Science Foundation of Jiangsu Province (BK20190782).

References

- 465 Balsamo, G., Beljaars, A., Scipal, K., Viterbo, P., van den Hurk, B., Hirschi, M., and Betts, A. K.: A Revised Hydrology for
the ECMWF Model: Verification from Field Site to Terrestrial Water Storage and Impact in the Integrated Forecast
System, *J. Hydrometeorol.*, 10, 623–643, <https://doi.org/10.1175/2008JHM1068.1>, 2009.
- Bamzai, A. S., and Shukla, J.: Relation between Eurasian Snow Cover, Snow Depth, and the Indian Summer Monsoon: An
Observational Study, *J. Climate*, 12, 3117–3132, [https://doi.org/10.1175/1520-0442\(1999\)012<3117:RBESCS>2.0.CO;2](https://doi.org/10.1175/1520-0442(1999)012<3117:RBESCS>2.0.CO;2),
1999.
- 470 Barnett, T. P., Dümenil, L., Schlese, U., Roeckner, E., and Latif, M.: The effect of Eurasian snow cover on regional and global
climate variations, *J. Atmos. Sci.*, 46, 661–686, [https://doi.org/10.1175/1520-0469\(1989\)046<0661:TEOESC>2.0.CO;2](https://doi.org/10.1175/1520-0469(1989)046<0661:TEOESC>2.0.CO;2),
1989.
- 475 [Chen, L., and Frauenfeld, O. W.: A comprehensive evaluation of precipitation simulations over China based on CMIP5
multimodel ensemble projections, *J. Geophys. Res. Atmos.*, 119, 5767–5786, <https://doi.org/10.1002/2013JD021190>,
2014.](#)
- Chen, X. N., Long, D., Hong, Y., Liang, S. L., and Hou, A. Z.: Observed radiative cooling over the Tibetan Plateau for the
past three decades driven by snow cover-induced surface albedo anomaly, *J. Geophys. Res. Atmos.*, 122, 6170–6185,
<https://doi.org/10.1002/2017jd026652>, 2017.

- Clark, M. P., and Serreze, M. C.: Effects of variations in east Asian snow cover on modulating atmospheric circulation over
480 the north pacific ocean, *J. Climate*, 13, 3700–3710, [https://doi.org/10.1175/1520-0442\(2000\)013<3700:eoviea>2.0.co;2](https://doi.org/10.1175/1520-0442(2000)013<3700:eoviea>2.0.co;2),
2000.
- Collins, W. D., Bitz, C. M., Blackmon, M. L., Bonan, G. B., Bretherton, C. S., Carton, J. A., Chang, P., Doney, S. C., Hack,
J. J., Henderson, T. B., Kiehl, J. T., Large, W. G., McKenna, D. S., Santer, B. D., and Smith, R. D.: The Community
Climate System Model version 3 (CCSM3), *J. Climate*, 19, 2122–2143, <https://doi.org/10.1175/jcli3761.1>, 2006.
- 485 de Andrade, F. M., Coelho, C. A. S., and Cavalcanti, I. F. A.: Global precipitation hindcast quality assessment of the
Subseasonal to Seasonal (S2S) prediction project models, *Clim. Dyn.*, 52, 5451–5475, <https://doi.org/10.1007/s00382-018-4457-z>, 2019.
- Dee, D. P., Uppala, S. M., Simmons, A. J., Berrisford, P., Poli, P., Kobayashi, S., Andrae, U., Balmaseda, M. A., Balsamo, G.,
Bauer, P., Bechtold, P., Beljaars, A. C. M., van de Berg, L., Bidlot, J., Bormann, N., Delsol, C., Dragani, R., Fuentes, M.,
490 Geer, A. J., Haimberger, L., Healy, S. B., Hersbach, H., Holm, E. V., Isaksen, L., Kallberg, P., Koehler, M., Matricardi,
M., McNally, A. P., Monge-Sanz, B. M., Morcrette, J. J., Park, B. K., Peubey, C., de Rosnay, P., Tavolato, C., Thepaut,
J. N., and Vitart, F.: The ERA-Interim reanalysis: configuration and performance of the data assimilation system, *Q. J. R.
Meteorolog. Soc.*, 137, 553–597, <https://doi.org/10.1002/qj.828>, 2011.
- Dirmeyer, P. A., Gentine, P., Ek, M. B., and Balsamo, G.: Chapter 8 - Land Surface Processes Relevant to Sub-seasonal to
495 Seasonal (S2S) Prediction, in: *Sub-Seasonal to Seasonal Prediction*, edited by: Robertson, A. W., and Vitart, F., Elsevier,
165–181, 2019.
- [Diro, G. T., and Lin, H.: Subseasonal Forecast Skill of Snow Water Equivalent and Its Link with Temperature in Selected
SubX Models, *Wea. Forecasting*, 35, 273-284, <https://doi.org/10.1175/WAF-D-19-0074.1>, 2020.](#)
- Dutra, E., Balsamo, G., Viterbo, P., Miranda, P. M. A., Beljaars, A., Schär, C., and Elder, K.: An Improved Snow Scheme for
500 the ECMWF Land Surface Model: Description and Offline Validation, *J. Hydrometeorol.*, 11, 899–916,
<https://doi.org/10.1175/2010JHM1249.1>, 2010.
- Ek, M. B., Mitchell, K. E., Lin, Y., Rogers, E., Grunmann, P., Koren, V., Gayno, G., and Tarpley, J. D.: Implementation of
Noah land surface model advances in the National Centers for Environmental Prediction operational mesoscale Eta model,
J. Geophys. Res. Atmos., 108, 8851, <https://doi.org/10.1029/2002JD003296>, 2003.
- 505 Fayad, A., Gascoin, S., Faour, G., López-Moreno, J. I., Drapeau, L., Page, M. L., and Escadafal, R.: Snow hydrology in
Mediterranean mountain regions: A review, *J. Hydrol.*, 551, 374–396, <https://doi.org/10.1016/j.jhydrol.2017.05.063>,
2017.
- Helfrich, S. R., McNamara, D., Ramsay, B. H., Baldwin, T., and Kasheta, T.: Enhancements to, and forthcoming developments
in the Interactive Multisensor Snow and Ice Mapping System (IMS), *Hydrol. Processes*, 21, 1576–1586,
510 <https://doi.org/10.1002/hyp.6720>, 2007.
- Henderson, G. R., Peings, Y., Furtado, J. C., and Kushner, P. J.: Snow–atmosphere coupling in the Northern Hemisphere, *Nat.
Clim. Change*, 8, 954–963, <https://doi.org/10.1038/s41558-018-0295-6>, 2018.

- Hong, S.-Y., and Lim, J.-O. J.: The WRF Single-Moment 6-Class Microphysics Scheme (WSM6), *Asia-Pac. J. Atmos. Sci.*, 42, 129–151, 2006.
- 515 Hong, S.-Y., Noh, Y., and Dudhia, J.: A new vertical diffusion package with an explicit treatment of entrainment processes, *Mon. Weather Rev.*, 134, 2318–2341, <https://doi.org/10.1175/mwr3199.1>, 2006.
- [Huffman, G. J., Adler, R. F., Bolvin, D. T., Gu, G., Nelkin, E. J., Bowman, K. P., Hong, Y., Stocker, E. F., and Wolff, D. B.: The TRMM multisatellite precipitation analysis \(TMPA\): Quasi-global, multiyear, combined-sensor precipitation estimates at fine scales, *J. Hydrometeorol.*, 8, 38–55, <https://doi.org/10.1175/jhm560.1>, 2007.](https://doi.org/10.1175/jhm560.1)
- 520 Immerzeel, W. W., Droogers, P., de Jong, S. M., and Bierkens, M. F. P.: Large-scale monitoring of snow cover and runoff simulation in Himalayan river basins using remote sensing, *Remote Sens. Environ.*, 113, 40–49, <https://doi.org/10.1016/j.rse.2008.08.010>, 2009.
- Jeelani, G., Feddema, J. J., van der Veen, C. J., and Stearns, L.: Role of snow and glacier melt in controlling river hydrology in Liddar watershed (western Himalaya) under current and future climate, *Water Resour. Res.*, 48, W12508, <https://doi.org/10.1029/2011WR011590>, 2012.
- 525 Jeong, J. H., Linderholm, H. W., Woo, S. H., Folland, C., Kim, B. M., Kim, S. J., and Chen, D. L.: Impacts of Snow Initialization on Subseasonal Forecasts of Surface Air Temperature for the Cold Season, *J. Climate*, 26, 1956–1972, <https://doi.org/10.1175/jcli-d-12-00159.1>, 2013.
- Kain, J. S.: The Kain-Fritsch convective parameterization: An update, *J. Appl. Meteorol.*, 43, 170–181, [https://doi.org/10.1175/1520-0450\(2004\)043<0170:tkcpau>2.0.co;2](https://doi.org/10.1175/1520-0450(2004)043<0170:tkcpau>2.0.co;2), 2004.
- 530 Kolstad, E. W.: Causal Pathways for Temperature Predictability from Snow Depth, *J. Climate*, 30, 9651–9663, <https://doi.org/10.1175/JCLI-D-17-0280.1>, 2017.
- Koren, V., Schaake, J., Mitchell, K., Duan, Q. Y., Chen, F., and Baker, J. M.: A parameterization of snowpack and frozen ground intended for NCEP weather and climate models, *J. Geophys. Res. Atmos.*, 104, 19569–19585, <https://doi.org/10.1029/1999JD900232>, 1999.
- 535 [Li, F., Orsolini, Y. J., Keenlyside, N., Shen, M. L., Counillon, F., and Wang, Y. G.: Impact of Snow Initialization in Subseasonal-to-Seasonal Winter Forecasts With the Norwegian Climate Prediction Model, *J. Geophys. Res. Atmos.*, 124, 10033–10048, <https://doi.org/10.1029/2019JD030903>, 2019.](https://doi.org/10.1029/2019JD030903)
- Li, Wei., Chen, J., Li, L., Chen, H., Liu, B., Xu, C.-Y., and Li, X.: Evaluation and Bias Correction of S2S Precipitation for Hydrological Extremes, *J. Hydrometeorol.*, 20, 1887–1906, <https://doi.org/10.1175/JHM-D-19-0042.1>, 2019.
- 540 Li, W., Guo, W., Hsu, P.-C., and Xue, Y.: Influence of the Madden–Julian oscillation on Tibetan Plateau snow cover at the intraseasonal time-scale, *Sci. Rep.*, 6, 30456, <https://doi.org/10.1038/srep30456>, 2016.
- Li, W., Guo, W., Qiu, B., Xue, Y., Hsu, P.-C., and Wei, J.: Influence of Tibetan Plateau snow cover on East Asian atmospheric circulation at medium-range time scales, *Nat. Commun.*, 9, 4243, <https://doi.org/10.1038/s41467-018-06762-5>, 2018.
- 545 Li, W., Qiu, B., Guo, W., Zhu, Z., and Hsu, P.-C.: Intraseasonal variability of Tibetan Plateau snow cover, *Int. J. Climatol.*, 40, 3451–3466 *in press*, <https://doi.org/10.1002/joc.6407>, 2020a.

- Li, W., Qiu, B., Guo, W., and Hsu, P.-C.: Rapid response of the East Asian trough to Tibetan Plateau snow cover, *Int. J. Climatol.*, in press, <https://doi.org/10.1002/joc.6618>, 2020b.
- Lin, H., and Wu, Z. W.: Contribution of the Autumn Tibetan Plateau Snow Cover to Seasonal Prediction of North American Winter Temperature, *J. Climate*, 24, 2801–2813, <https://doi.org/10.1175/2010jcli3889.1>, 2011.
- Lin, P., Wei, J., Yang, Z. L., Zhang, Y., and Zhang, K.: Snow data assimilation-constrained land initialization improves seasonal temperature prediction, *Geophys. Res. Lett.*, 43, 11423–411432, <https://doi.org/10.1002/2016GL070966>, 2016.
- Mariotti, A., Ruti, P. M., and Rixen, M.: Progress in subseasonal to seasonal prediction through a joint weather and climate community effort, *npj Clim. Atmos. Sci.*, 1, 4, <https://doi.org/10.1038/s41612-018-0014-z>, 2018.
- 555 Orsolini, Y. J., Senan, R., Balsamo, G., Doblas-Reyes, F. J., Vitart, F., Weisheimer, A., Carrasco, A., and Benestad, R. E.: Impact of snow initialization on sub-seasonal forecasts, *Clim. Dyn.*, 41, 1969–1982, <https://doi.org/10.1007/s00382-013-1782-0>, 2013.
- [Orsolini, Y., Wegmann, M., Dutra, E., Liu, B., Balsamo, G., Yang, K., de Rosnay, P., Zhu, C., Wang, W., Senan, R., and Arduini, G.: Evaluation of snow depth and snow cover over the Tibetan Plateau in global reanalyses using in situ and satellite remote sensing observations, *The Cryosphere*, 13, 2221–2239, https://doi.org/10.5194/tc-13-2221-2019, 2019.](https://doi.org/10.5194/tc-13-2221-2019)
- 560 Robertson, A. W., Kumar, A., Peña, M., and Vitart, F.: Improving and Promoting Subseasonal to Seasonal Prediction, *Bull. Am. Meteorol. Soc.*, 96, ES49–ES53, <https://doi.org/10.1175/BAMS-D-14-00139.1>, 2014.
- Schmitt Quedi, E., and Mainardi Fan, F.: Sub seasonal streamflow forecast assessment at large-scale basins, *J. Hydrol.*, 584, 124635, <https://doi.org/10.1016/j.jhydrol.2020.124635>, 2020.
- 565 [Schneider, U., Becker, A., Finger, P., Meyer-Christoffer, A., Rudolf, B., and Ziese, M.: GPCP full data reanalysis version 6.0 at 0.5: monthly land-surface precipitation from rain-gauges built on GTS-based and historic data, *GPCC Data Rep.*, https://doi.org/10.5676/DWD_GPCC/FD_M_V7_100, 2011.](https://doi.org/10.5676/DWD_GPCC/FD_M_V7_100)
- Senan, R., Orsolini, Y. J., Weisheimer, A., Vitart, F., Balsamo, G., Stockdale, T. N., Dutra, E., Doblas-Reyes, F. J., and Basang, D.: Impact of springtime Himalayan-Tibetan Plateau snowpack on the onset of the Indian summer monsoon in coupled seasonal forecasts, *Clim. Dyn.*, 47, 2709–2725, <https://doi.org/10.1007/s00382-016-2993-y>, 2016.
- 570 Song, L., and Wu, R.: Intraseasonal Snow Cover Variations Over Western Siberia and Associated Atmospheric Processes, *J. Geophys. Res. Atmos.*, 124, 8994–9010, <https://doi.org/10.1029/2019JD030479>, 2019.
- Song, L., Wu, R. G., and An, L.: Different Sources of 10-to 30-day Intraseasonal Variations of Autumn Snow over Western and Eastern Tibetan Plateau, *Geophys. Res. Lett.*, 46, 9118–9125, <https://doi.org/10.1029/2019gl083852>, 2019.
- 575 [Su, F., Duan, X., Chen, D., Hao, Z., and Cuo, L.: Evaluation of the Global Climate Models in the CMIP5 over the Tibetan Plateau, *J. Climate*, 26, 3187–3208, https://doi.org/10.1175/JCLI-D-12-00321.1, 2013.](https://doi.org/10.1175/JCLI-D-12-00321.1)
- Suriano, Z. J., and Leathers, D. J.: Great Lakes Basin Snow-Cover Ablation and Synoptic-Scale Circulation, *J. Appl. Meteorol. and Climatology*, 57, 1497–1510, <https://doi.org/10.1175/jamc-d-17-0297.1>, 2018.

- 580 Vitart, F.: Madden–Julian Oscillation prediction and teleconnections in the S2S database, *Q. J. R. Meteorolog. Soc.*, 143, 2210–2220, <https://doi.org/10.1002/qj.3079>, 2017.
- Vitart, F., Ardilouze, C., Bonet, A., Brookshaw, A., Chen, M., Codorean, C., Déqué, M., Ferranti, L., Fucile, E., Fuentes, M., Hendon, H., Hodgson, J., Kang, H. S., Kumar, A., Lin, H., Liu, G., Liu, X., Malguzzi, P., Mallas, I., Manoussakis, M., Mastrangelo, D., MacLachlan, C., McLean, P., Minami, A., Mladek, R., Nakazawa, T., Najm, S., Nie, Y., Rixen, M.,
585 Robertson, A. W., Ruti, P., Sun, C., Takaya, Y., Tolstykh, M., Venuti, F., Waliser, D., Woolnough, S., Wu, T., Won, D. J., Xiao, H., Zaripov, R., and Zhang, L.: The Subseasonal to Seasonal (S2S) Prediction Project Database, *Bull. Am. Meteorol. Soc.*, 98, 163–173, <https://doi.org/10.1175/BAMS-D-16-0017.1>, 2016.
- Wang, C., Yang, K., Li, Y., Wu, D., and Bo, Y.: Impacts of Spatiotemporal Anomalies of Tibetan Plateau Snow Cover on Summer Precipitation in Eastern China, *J. Climate*, 30, 885–903, <https://doi.org/10.1175/JCLI-D-16-0041.1>, 2017.
- 590 Wang, T., Peng, S., Oettle, C., and Ciais, P.: Spring snow cover deficit controlled by intraseasonal variability of the surface energy fluxes, *Environ. Res. Lett.*, 10, 024018, <https://doi.org/10.1088/1748-9326/10/2/024018>, 2015.
- White, C. J., Carlsen, H., Robertson, A. W., Klein, R. J. T., Lazo, J. K., Kumar, A., Vitart, F., Coughlan de Perez, E., Ray, A. J., Murray, V., Bharwani, S., MacLeod, D., James, R., Fleming, L., Morse, A. P., Eggen, B., Graham, R., Kjellström, E., Becker, E., Pegion, K. V., Holbrook, N. J., McEvoy, D., Depledge, M., Perkins-Kirkpatrick, S., Brown, T. J., Street, R.,
595 Jones, L., Remenyi, T. A., Hodgson-Johnston, I., Buontempo, C., Lamb, R., Meinke, H., Arheimer, B., and Zebiak, S. E.: Potential applications of subseasonal-to-seasonal (S2S) predictions, *Meteorol. Appl.*, 24, 315–325, <https://doi.org/10.1002/met.1654>, 2017.
- Wu, R. G., and Kirtman, B. P.: Observed relationship of spring and summer East Asian rainfall with winter and spring Eurasian snow, *J. Climate*, 20, 1285–1304, <https://doi.org/10.1175/jcli4068.1>, 2007.
- 600 Wu, T., Song, L., Li, W., Wang, Z., Zhang, H., Xin, X., Zhang, Y., Zhang, L., Li, J., Wu, F., Liu, Y., Zhang, F., Shi, X., Chu, M., Zhang, J., Fang, Y., Wang, F., Lu, Y., Liu, X., Wei, M., Liu, Q., Zhou, W., Dong, M., Zhao, Q., Ji, J., Li, L., and Zhou, M.: An overview of BCC climate system model development and application for climate change studies, *J. Meteorolog. Res.*, 28, 34–56, <https://doi.org/10.1007/s13351-014-3041-7>, 2014.
- Wu, T., and Wu, G.: An empirical formula to compute snow cover fraction in GCMs, *Adv. Atmos. Sci.*, 21, 529–535,
605 <https://doi.org/10.1007/BF02915720>, 2004.
- Wu, T. W., and Qian, Z. A.: The relation between the Tibetan winter snow and the Asian summer monsoon and rainfall: An observational investigation, *J. Climate*, 16, 2038–2051, [https://doi.org/10.1175/1520-0442\(2003\)016<2038:trbttw>2.0.co;2](https://doi.org/10.1175/1520-0442(2003)016<2038:trbttw>2.0.co;2), 2003.
- Wulff, C. O., and Domeisen, D. I. V.: Higher Subseasonal Predictability of Extreme Hot European Summer Temperatures as
610 Compared to Average Summers, *Geophys. Res. Lett.*, 46, 11520–11529, <https://doi.org/10.1029/2019GL084314>, 2019.
- Xiao, Z. X., and Duan, A. M.: Impacts of Tibetan Plateau Snow Cover on the Interannual Variability of the East Asian Summer Monsoon, *J. Climate*, 29, 8495–8514, <https://doi.org/10.1175/jcli-d-16-0029.1>, 2016.

- Yang, J., Jiang, L., Ménard, C. B., Luo, K., Lemmetyinen, J., and Pulliainen, J.: Evaluation of snow products over the Tibetan Plateau, *Hydrol. Processes*, 29, 3247–3260, <https://doi.org/10.1002/hyp.10427>, 2015.
- 615 Yang, J., Zhu, T., Gao, M., Lin, H., Wang, B., and Bao, Q.: Late-July Barrier for Subseasonal Forecast of Summer Daily Maximum Temperature Over Yangtze River Basin, *Geophys. Res. Lett.*, 45, 12,610–612,615, <https://doi.org/10.1029/2018GL080963>, 2018.
- You, Q., Wu, T., Shen, L., Pepin, N., Zhang, L., Jiang, Z., Wu, Z., Kang, S., and AghaKouchak, A.: Review of snow cover variation over the Tibetan Plateau and its influence on the broad climate system, *Earth Sci. Rev.*, 201, 103043, <https://doi.org/10.1016/j.earscirev.2019.103043>, 2020.
- 620 [Zhang, F., Ren, H., Miao, L., Lei, Y., and Duan, M.: Simulation of Daily Precipitation from CMIP5 in the Qinghai-Tibet Plateau, *SOLA*, 15, 68–74, <https://doi.org/10.2151/sola.2019-014>, 2019.](https://doi.org/10.2151/sola.2019-014)
- Zhang, G., Xie, H., Yao, T., Liang, T., and Kang, S.: Snow cover dynamics of four lake basins over Tibetan Plateau using time series MODIS data (2001-2010), *Water Resour. Res.*, 48, W10529, <https://doi.org/10.1029/2012wr011971>, 2012.
- 625 Zhang, L. L., Su, F. G., Yang, D. Q., Hao, Z. C., and Tong, K.: Discharge regime and simulation for the upstream of major rivers over Tibetan Plateau, *J. Geophys. Res. Atmos.*, 118, 8500–8518, <https://doi.org/10.1002/jgrd.50665>, 2013.
- Zhang, T. J.: Influence of the seasonal snow cover on the ground thermal regime: An overview, *Rev. Geophys.*, 43, RG4002, <https://doi.org/10.1029/2004rg000157>, 2005.
- 630 [Zhang, Y., and Li, J.: Impact of moisture divergence on systematic errors in precipitation around the Tibetan Plateau in a general circulation model, *Clim. Dyn.*, 47, 2923–2934, <https://doi.org/10.1007/s00382-016-3005-y>, 2016.](https://doi.org/10.1007/s00382-016-3005-y)
- Zhang, Y., Zou, T., and Xue, Y.: An Arctic-Tibetan Connection on Subseasonal to Seasonal Time Scale, *Geophys. Res. Lett.*, 46, 2790–2799, <https://doi.org/10.1029/2018GL081476>, 2019.

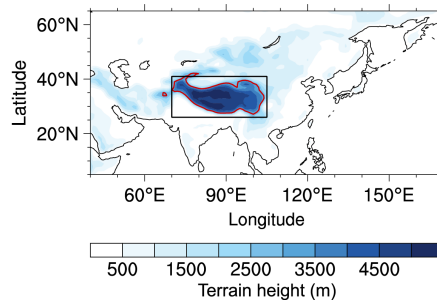


Figure 1. The location and topography of the Tibetan Plateau. Shading shows topography (unit: m). The black rectangle shows the region within 26–41°N and 70–105°E. The red contour marks altitudes at 3000 m. The Tibetan Plateau area, which is the focus of this study is the region within the black rectangle at an altitude of greater than 3000 m. This figure also shows the simulation domain for numerical experiments in this study.

10

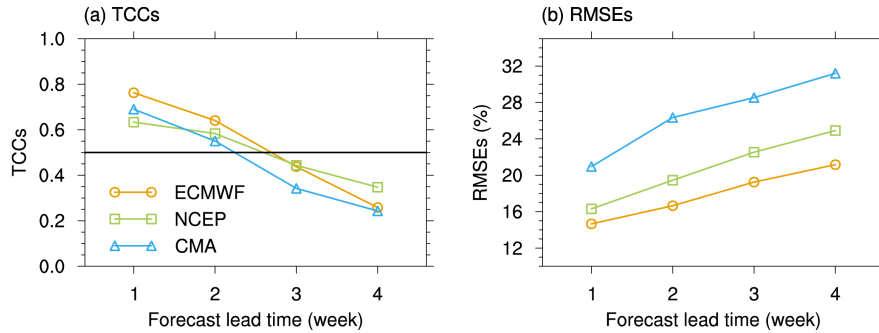
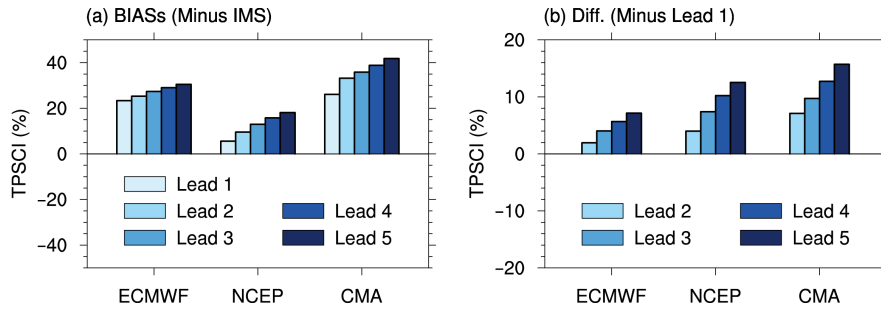


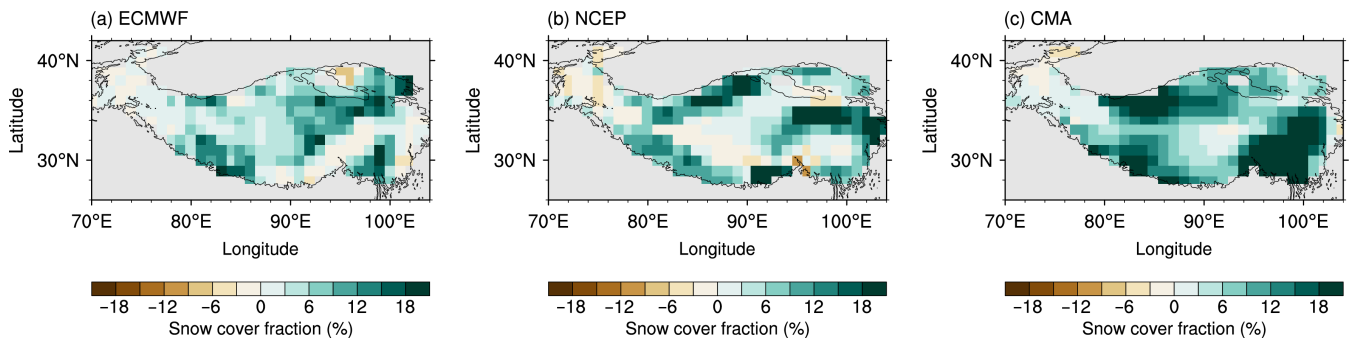
Figure 2. Prediction skill of the Tibetan Plateau snow cover (TPSC) index in the S2S models during wintertime. **(a)** The temporal correlation coefficients (TCCs; y-axis) between the observed TPSC index and the predicted TPSC index in the ECMWF (orange line), NCEP (green line) and CMA (blue line) models during winter. The x-axis represents the forecast lead time (unit: week). A good prediction skill has a TCC that is greater than 0.5 (marked by black line). **(b)** is similar to (a) but is for the root-mean-square errors (RMSEs; y-axis, unit: %).

20



25 **Figure 3.** (a) The multiyear wintertime mean seasonal cycle for the weekly biases of Tibetan Plateau snow cover (TPSC) index (unit: %) in (a) ECMWF, (b) NCEP, and (c) CMA forecasts against those in the Interactive Multisensor Snow and Ice Mapping System (IMS) snow cover analysis. (b) The black lines represent the TPSC index in the observation; the red or blue lines represent the TPSC index in the forecast models for different lead times (in week); see legend in (a). The x axis represents the first day of each week in the seasonal cycle.

30 **Figure 4.** Differences in the multiyear wintertime mean seasonal cycle for the weekly Tibetan Plateau snow cover index (unit: %) TPSC index between forecasts with a lead of 2–5 weeks and forecasts with a lead of 1 week in (a) ECMWF, (b) NCEP, and (c) CMA each model. The x axis represents the first day of each week in the seasonal cycle.



35 **Figure 4.** Differences in the multiyear wintertime mean Tibetan Plateau snow cover fraction (unit: %) between forecasts with a lead of 4 weeks and forecasts with a lead of 1 week in (a) ECMWF, (b) NCEP and (c) CMA.

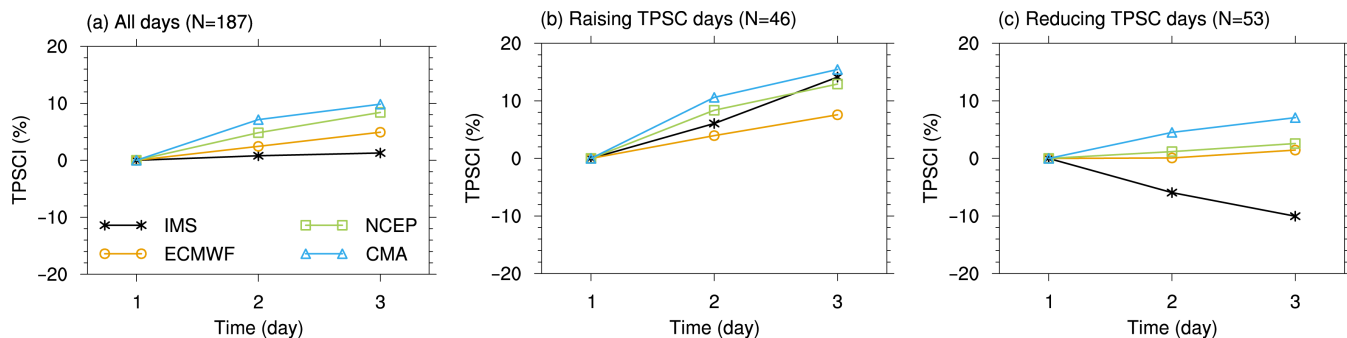


Figure 5. Composites of the Tibetan Plateau snow cover index (unit: %) for (a) all cases, (b) increasing TPSC cases, and (c) decreasing TPSC cases. Black lines, orange lines, green lines and blue lines represent composites in the observation, ECMWF, NCEP, and CMA, respectively; see legend in (a). The x -axis represents the number of weeks in the cases for the composites, which are also forecast lead times (unit: week). The “N” in the title of each plot indicates the number of cases for the composite.

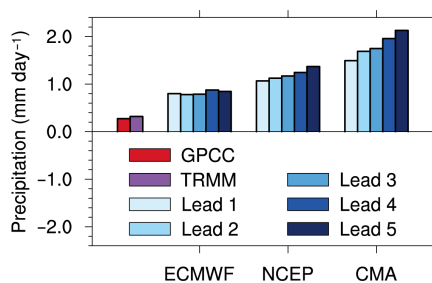


Figure 6. The multiyear wintertime mean precipitation over the Tibetan Plateau (unit: mm day⁻¹) for the observations and forecasts in each model.

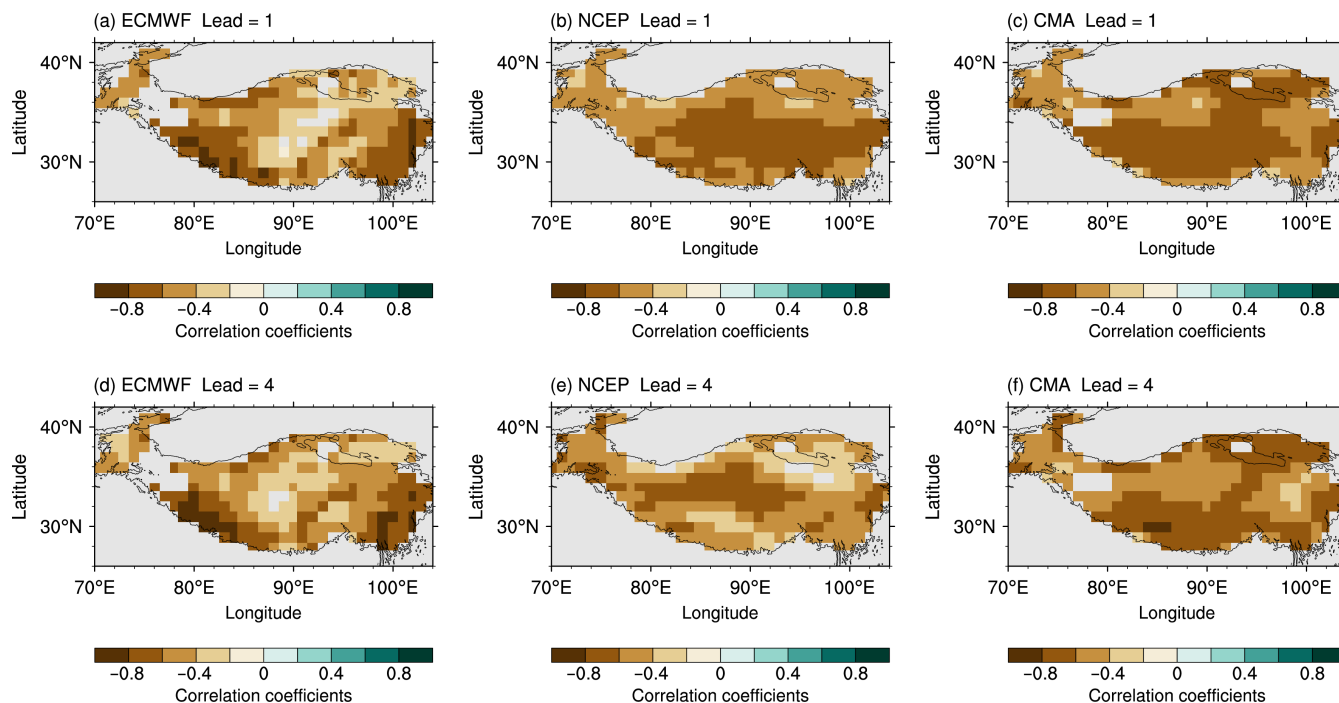


Figure 7. Spatial pattern of correlations between the snow cover fraction and the surface air temperature with a lead of 1 week in (a) ECMWF, (b) NCEP and (c) CMA. Only significant correlations at the 0.01 level are displayed. (d)–(f) is similar to (a)–(c) but for forecasting with a lead of 4 weeks.

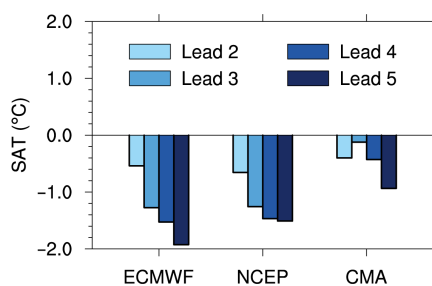


Figure 68. Differences in the multiyear wintertime mean seasonal cycle for weekly surface air temperature over the Tibetan Plateau (unit: °C) between forecasts with a lead of 2–5 weeks and forecasts with a lead of 1 week in (a) ECMWF, (b) NCEP, and (c) CMA each model. The x-axis represents the first day of each week in the seasonal cycle.

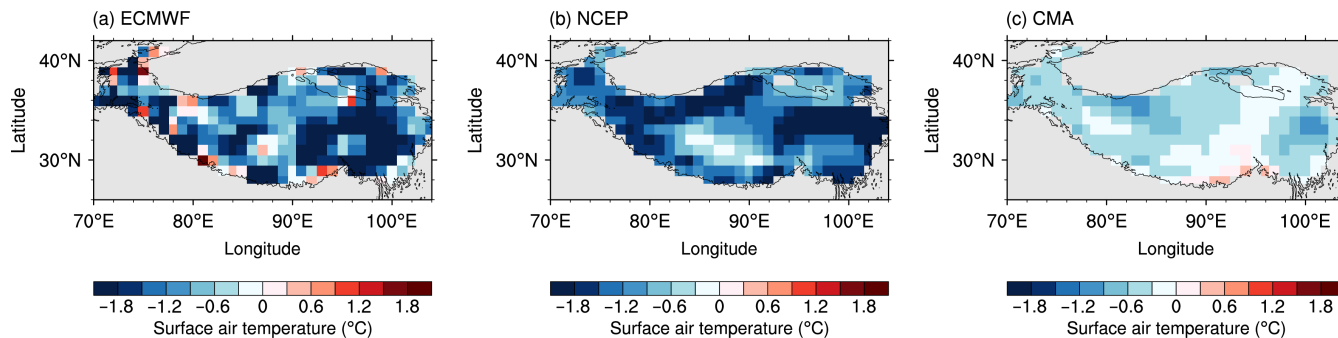


Figure 9. Differences in the multiyear wintertime mean surface air temperature over the Tibetan Plateau (unit: °C) between forecasts with a lead of 4 weeks and forecasts with a lead of 1 week in (a) ECMWF, (b) NCEP and (c) CMA.

75

80

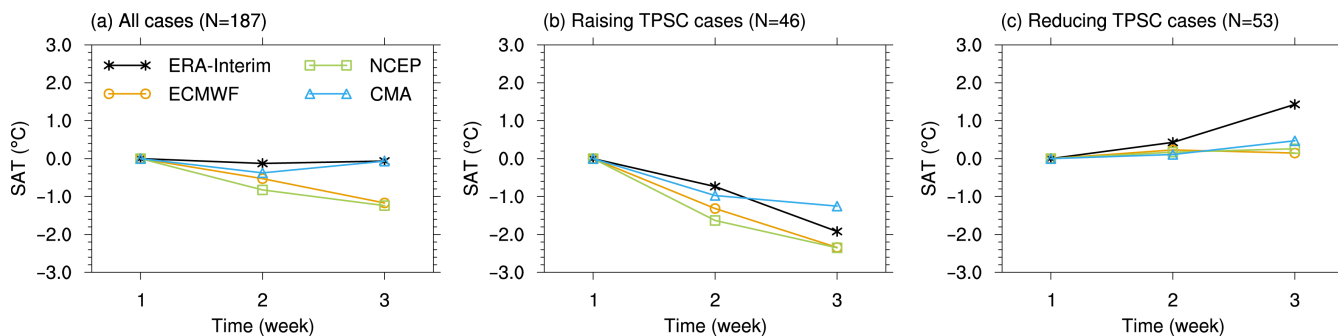


Figure 10. Composites of surface air temperature over the Tibetan Plateau (unit: °C) for (a) all cases, (b) increasing TPSC cases, and (c) decreasing TPSC cases. Black lines, orange lines, green lines, blue lines and black lines represent composites in observation, ECMWF, NCEP, and CMA, respectively; see legend in (a). The x-axis represents the number of weeks in the cases for the composites, which are also forecast lead times (unit: week). The “N” in the title of each plot indicates the number of cases for the composite.

85

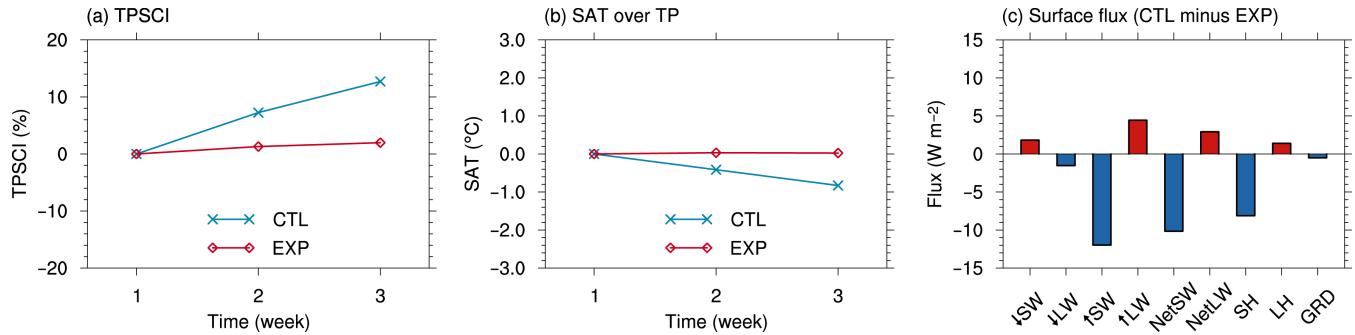


Figure 11. Sensitivity of SAT and surface energy balance to TPSC biases in the numerical experiments. (a) TPSCI and (b) SAT over TP in CTL (blue lines) and EXP (red lines) runs. The units of TPSCI and SAT are % and °C. The x-axis represents the number of weeks lagging the start of the model initial date (unit: week). (c) The difference in the surface energy balance between the CTL and EXP (CTL minus EXP) at 3 weeks in the numerical experiments. The terms from left to right are downward shortwave radiation (\downarrow SW), downward longwave radiation (\downarrow LW), upward shortwave radiation (\uparrow SW), upward longwave radiation (\uparrow LW), net shortwave radiation (NetSW), net longwave radiation (NetLW), sensible heat flux (SH), latent heat flux (LH) and ground heat flux (GRD) at the surface over the TP, respectively (unit: W m^{-2}).

95

100

Table 1. The proportion of increasing (decreasing) weeks in the observations and forecast models with different lead times (in weeks).

	Observation/Lead=2	Lead=3	Lead=4	Lead=5
IMS	50.3% (49.7%)			
ECMWF	72.7% (27.3%)	77.0% (23.0%)	70.6% (29.4%)	69.0% (31.0%)
NCEP	77.5% (22.5%)	69.5% (30.5%)	64.7% (35.3%)	55.1% (44.9%)
CMA	86.6% (13.4%)	67.4% (32.6%)	72.2% (27.8%)	79.7% (20.3%)

105